

 Open access • Posted Content • DOI:10.1101/096289

Natural diversity of the malaria vector *Anopheles gambiae* — Source link

Alistair Miles, Nicholas J. Harding, Giordano Bottà, Chris S Clarkson ...+57 more authors

Institutions: Wellcome Trust Sanger Institute, University of Oxford, University of Montana, Rutgers University ...+14 more institutions

Published on: 22 Dec 2016 - bioRxiv (Cold Spring Harbor Laboratory)

Topics: Anopheles gambiae, Mosquito control and Malaria

Related papers:

- [Natural diversity of the malaria vector *Anopheles gambiae*](#)
- [Concerning RNA-guided gene drives for the alteration of wild populations](#)
- [A CRISPR-Cas9 gene drive system targeting female reproduction in the malaria mosquito vector *Anopheles gambiae*](#)
- [Evolution of Resistance Against CRISPR/Cas9 Gene Drive.](#)
- [Requirements for effective malaria control with homing endonuclease genes](#)

Share this paper:    

View more about this paper here: <https://typeset.io/papers/natural-diversity-of-the-malaria-vector-anopheles-gambiae-94b3rzje5e>

1 Natural diversity of the malaria vector

2 *Anopheles gambiae*

3 The *Anopheles gambiae* 1000 Genomes Consortium*

4 **The sustainability of malaria control in Africa is threatened by rising levels of insecticide resistance,**
5 **and new tools to prevent malaria transmission are urgently needed. To gain a better understanding of**
6 **the mosquito populations that transmit malaria, we sequenced the genomes of 765 wild specimens of**
7 ***Anopheles gambiae* and *Anopheles coluzzii* sampled from 15 locations across Africa. The data reveal**
8 **high levels of genetic diversity, with over 50 million single nucleotide polymorphisms across the 230**
9 **Mbp genome. We observe complex patterns of population structure and marked variations in local**
10 **population size, some of which may be due at least in part to malaria control interventions.**
11 **Insecticide resistance genes show strong signatures of recent selection associated with multiple**
12 **independent mutations spreading over large geographical distances and between species. The genetic**
13 **variability of natural populations substantially reduces the target space for novel gene-drive strategies**
14 **for mosquito control. This large dataset provides a foundation for tracking the emergence and spread**
15 **of insecticide resistance and developing new vector control tools.**

16 Blood-sucking mosquitoes of the *Anopheles gambiae* species complex exert a heavy toll on human
17 health, being the principal vectors of *Plasmodium falciparum* malaria in Africa. Increased use of
18 insecticide-treated bed nets (ITNs) and other methods of vector control have led to substantial
19 reductions in the burden of malaria in Africa over the past 15 years^{1,2}. However, these gains could be
20 reversed by insecticide resistance that is rapidly spreading across the continent^{3,4} and by behavioural

* Lists of participants and their affiliations appear at the end of the paper

21 adaptations which cause mosquitoes to avoid contact with insecticides⁵. New insecticides are being
22 developed for use in public health^{6,7} and there is growing support for gene drive technologies for
23 malaria vector control⁸⁻¹⁰. However, relatively little is known about natural genetic diversity of
24 *Anopheles* vector species, or the evolutionary and demographic processes that allow adaptive mutations
25 to emerge and spread through mosquito populations. This knowledge is needed to maximize the
26 efficacy and active lifespan of new insecticides and to design gene drive systems that work in the field.

27 The *Anopheles gambiae* 1000 Genomes Project[†] (Ag1000G) was established to discover natural genetic
28 variation within this species complex, and to provide a fundamental resource for applied research into
29 malaria vector control. Here we report on the first phase of the project, that has generated genome-
30 wide data on nucleotide variation in 765 wild-caught mosquitoes, sampled from 15 locations in 8
31 countries spanning a variety of ecological settings, including rainforest, inland savanna and coastal
32 biomes (Supplementary Fig. 1). We sampled the two major malaria vector species within the species
33 complex, *Anopheles gambiae sensu stricto* and *Anopheles coluzzii*, which are morphologically
34 indistinguishable and often sympatric but may differ in geographical range¹¹, larval ecology¹²,
35 behaviour¹³ and strategies for surviving the dry season¹⁴. *An. gambiae* and *An. coluzzii* have been
36 classified as different species¹⁵ because they are genetically distinct¹⁶⁻¹⁸. However, although they
37 undergo assortative mating¹⁹, reproductive isolation is incomplete: hybrids are viable and fertile, and
38 there is evidence for hybridization in nature varying over space²⁰⁻²² and time²³, creating opportunities
39 for gene flow between species^{24,25}. The diversity of sampling in this project phase over geography,
40 ecology and species is not exhaustive, but does provide a broad platform from which to explore the
41 factors shaping mosquito population variation, evolution and speciation.

[†] <http://www.malariagen.net/ag1000g>

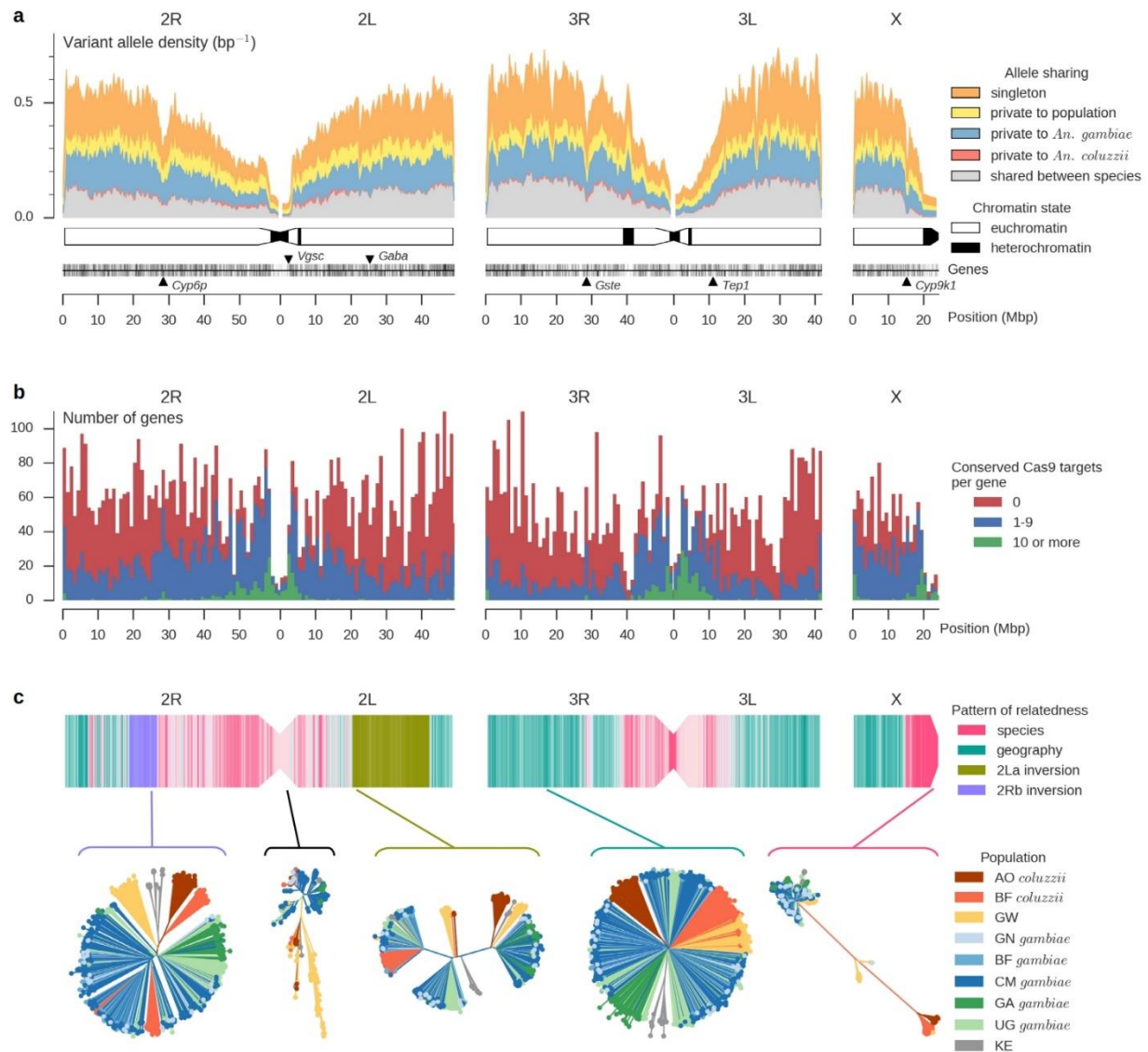


Figure 1. Patterns of genomic variation. **a**, Density of variant alleles in non-overlapping 200 kbp windows over the genome, computed as the number of variant alleles discovered in SNPs passing all quality filters divided by the number of accessible positions. Schematic of chromosomes below shows regions of heterochromatin²⁶. **b**, Genomic distribution of genes containing conserved regions that could be targeted by CRISPR/Cas9 gene drive. **c**, Variations in the pattern of relatedness between individual mosquitoes over the genome. The upper part of the plot shows a schematic of the three chromosomes painted using colours to represent the major pattern of relatedness within non-overlapping 100 kbp windows. Below, neighbour-joining trees are shown from a selection of genomic windows that are representative of the four major patterns of relatedness found, as well as for the window spanning the *Vgsc* gene on chromosome arm 2L which has a unique pattern of relatedness. The strength of colour indicates the strength of the correlation with the closest major pattern. AO = Angola; BF = Burkina Faso; GW = Guinea-Bissau; GN = Guinea; CM = Cameroon; GA = Gabon; UG = Uganda; KE = Kenya. Species status is uncertain for GW and KE populations.

42 Genomic variation

43 We used the Illumina HiSeq platform to perform whole genome deep sequencing on individual
44 mosquitoes. After removing samples with low coverage (<14X) we analyzed data on 765 wild-caught
45 specimens and a further 80 specimens comprising parents and progeny from 4 lab crosses
46 (Supplementary Fig. 1). Sequence reads were aligned against the AgamP3 reference genome²⁷ and
47 putative single nucleotide polymorphisms (SNPs) were called from the alignments^{28,29} (Supplementary
48 Text). The alignments were also used to identify genome regions accessible to SNP calling, where short
49 reads could be uniquely mapped and there was minimal evidence for structural variation^{30,31}. We
50 classified 61% (141 Mbp) of the AgamP3 chromosomal reference sequence as accessible, including 91%
51 (18 Mbp) of coding and 59% (123 Mbp) of non-coding positions (Supplementary Fig. 2A). Mendelian
52 errors in the crosses were used to guide the design of filters to remove poor quality variant calls. In total
53 52,525,957 SNPs passed all quality filters. We then used statistical phasing, combined with information
54 from sequence reads³², to estimate haplotypes for all wild-caught individuals. To assess the reliability of
55 this dataset, we performed capillary sequencing of 5 genes, from which we estimated a false discovery
56 rate of less than 1% and a sensitivity of 94% to detect SNPs within the accessible genome. We also
57 obtained >98% concordance of heterozygous genotype calls in comparisons with capillary sequence data
58 and >97% concordance in a second validation experiment using genotyping by primer-extension mass
59 spectrometry³³. We assessed phasing performance for wild-caught individuals by comparison with
60 haplotypes generated from the crosses (Supplementary Fig. 3A) and from male X chromosome
61 haplotypes, obtaining results comparable to human sequencing studies³² (Supplementary Fig. 3B).
62 Individual mosquitoes carried between 1.7 and 2.7 million variant alleles, with no systematic difference
63 observed between species (Supplementary Fig. 4A). SNPs were mostly biallelic, but 21% had three or
64 more alleles, and we discovered one variant allele every 2.2 bases of the accessible genome on average.

65 Variant allele density was similar on all chromosomes but markedly reduced in pericentromeric regions,
66 as expected due to linked selection in regions of low recombination^{34–36} (Fig. 1A). Gene structure had a
67 strong influence on nucleotide diversity, with the lowest diversity observed at non-degenerate coding
68 positions and at the dinucleotide core of intron splice sites, as expected due to purifying selection on
69 deleterious functional mutations (Supplementary Fig. 4B). We also found that diversity at fourfold
70 degenerate codon positions and within short introns was twice the level found in longer introns and
71 intergenic regions, similar to studies in *Drosophila*³⁷ and *Heliconius*³⁸, indicating that most non-coding
72 sequence is under moderate selective constraint.

73 Since the advent of efficient genome editing using the CRISPR/Cas9 system³⁹, the push to implement
74 gene drive in *Anopheles* to carry out population suppression¹⁰ or replacement⁹ has intensified. However,
75 variants within the short ~21 bp Cas9 target site represent potential resistance alleles, and thus the
76 sheer density of SNPs could negatively impact successful deployment of gene drive in *Anopheles*. We
77 explored the accessible coding genome for CRISPR/Cas9 target sites and found viable targets in 10,711
78 of 12,901 annotated genes (Supplementary Text). However, only 5,012 genes retained at least one
79 viable target after accounting for variation within target sites, and this is likely to worsen with further
80 population sampling (Supplementary Text). These possible target genes were spread non-uniformly
81 across the genome, falling predominantly in pericentromeric regions, where levels of variation were
82 lower (Fig. 1B). The evolution of resistance to gene drive will be caused both by natural variation and by
83 the DNA repair machinery itself, and therefore drive-based methods are unlikely to work unless multiple
84 genes and multiple sites within each gene are targeted. To that end, we identified 544 genes that each
85 contain at least 10 non-overlapping conserved target sites, including 9 putative sterility genes¹⁰
86 (Supplementary Text). The genome sequences presented here are a valuable resource for prioritizing
87 genes and designing gene drive strategies that will be effective in natural populations.

88 Population structure and gene flow

89 Analysis of genetic structure provides a foundation for studying the evolutionary and demographic
90 history of populations, and for understanding how genetic variants move between populations. We are
91 particularly interested in gene flow across geographical ranges via migration, and gene flow between
92 species via hybridization, as both can play a role in the spread of medically-important variants, including
93 insecticide resistance mutations^{24,25} and introduced genetic modifications. Previous studies of the
94 *Anopheles gambiae* complex have shown that phylogenetic relationships can vary dramatically between
95 different genomic regions^{24,25,40–42}. We therefore began by computing genetic distances between
96 individual mosquitoes and constructing neighbour-joining (NJ) trees within non-overlapping genomic
97 windows of 100,000 accessible bases (Fig. 1C). By analyzing the correlation between genetic distances in
98 different genomic windows, we identified four major patterns of relatedness, systematically associated
99 with different genomic regions. Within pericentromeric regions of chromosomes X, 3, and arm 2R,
100 mosquitoes segregated into two distinct and widely separated clusters, largely corresponding to the two
101 species as determined by conventional molecular diagnostics^{18,43}. Individuals from coastal Guinea-
102 Bissau, where reproductive isolation between species is believed to have broken down^{20–22}, were an
103 exception, being found in both clusters with poor correspondence to species assignments, as well as in
104 an intermediate cluster. The large chromosomal inversions⁴⁴ 2La and 2Rb were each associated with a
105 distinct pattern of relatedness, as expected if gene flow is limited by reduced recombination between
106 inversion karyotypes^{42,45}. Genetic structure was weak throughout most of the remainder of the genome,
107 with some separation of populations at the extremes of the geographical range (Angola, Kenya), but no
108 evidence of clustering by species. In addition to these four major patterns of relatedness, we found
109 other distinct patterns within some isolated genome regions, including windows near the voltage-gated
110 sodium channel (*Vgsc*) gene⁴⁶, a known locus of resistance to DDT and pyrethroid insecticides^{24,25}.

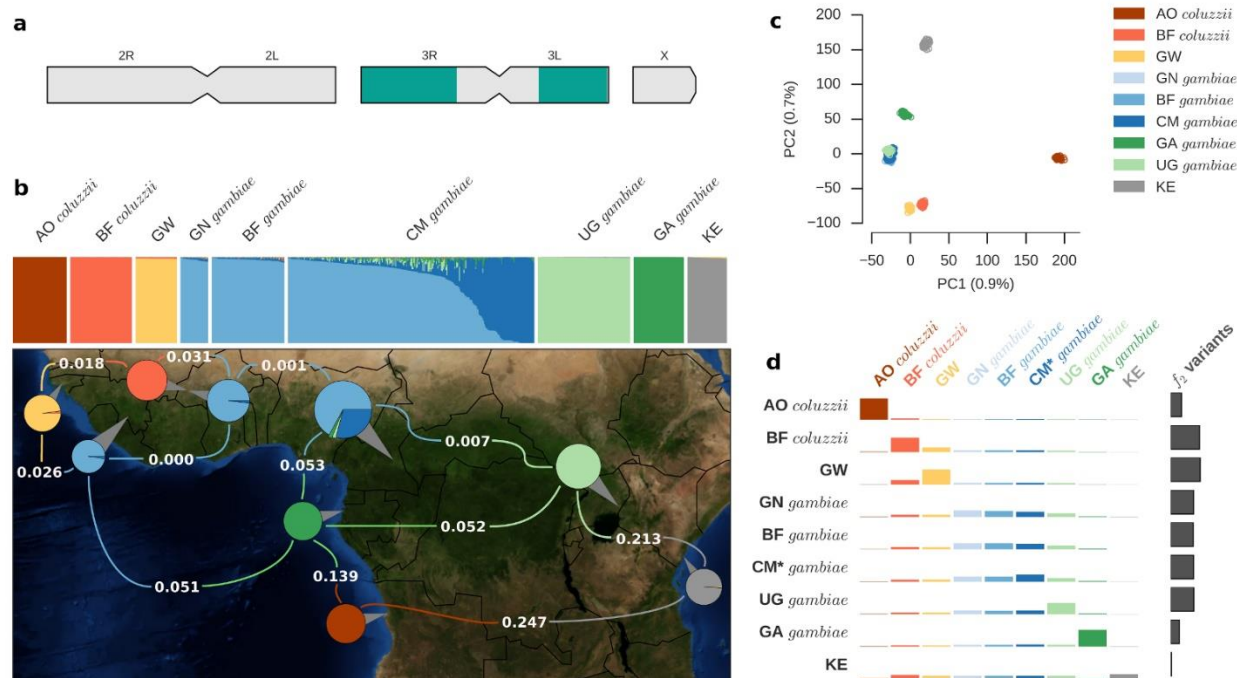


Figure 2. Geographical population structure. **a**, Schematic showing regions of the genome used for analyses of geographical population structure highlighted in turquoise. **b**, ADMIXTURE and allele frequency differentiation (F_{ST}). The upper panel depicts each of the 765 wild-caught mosquitoes as a vertical bar, painted by the proportion of the genome inherited from each of $K=8$ inferred ancestral populations. Pie charts on the map depict the same inferred ancestral proportions summed over all individuals for each of 9 groups defined by species and country of origin; grey pointers attached to each pie chart show the sampling location. Average F_{ST} values are overlaid in white for selected pairs of populations. **c**, Principal components analysis. Each marker represents an individual mosquito, projected onto the first two principal components of genetic variation. **d**, Allele sharing in f_2 variants. The height of the coloured bars represent the probability of sharing a doubleton allele between two populations. Heights are normalized row-wise for each population. Grey bars at the end of each row depict the total number of doubletons found in individuals from the given population. CM^* = Cameroon savanna sampling site only.

111 These other patterns were characterized by short genetic distances between individuals from different
 112 populations and species, indicating the influence of recent selective sweeps and adaptive gene flow.
 113 To investigate the influence of geography on population structure, we analyzed data from Chromosome
 114 3, which is free from high frequency polymorphic inversions⁴⁴ (Fig. 2A). We used ADMIXTURE to model
 115 each individual as a mixture deriving from K ancestral populations⁴⁷ and compared with results from
 116 principal components analysis (PCA) and allele frequency differentiation (F_{ST}) (Supplementary Text; Fig.
 117 2B, 2C; Supplementary Figs. 5, 6). All analyses supported five major ancestral populations,
 118 corresponding to: (i) Guinea, Burkina Faso, Cameroon and Uganda *An. gambiae*; (ii) Gabon *An. gambiae*;
 119 (iii) Kenya; (iv) Angola *An. coluzzii*; (v) Burkina Faso *An. coluzzii* and Guinea-Bissau. These results are

120 consistent with previous evidence that the Congo Basin tropical rainforest and the East African Rift Zone
121 are natural barriers to gene flow^{44,48–51}. Within each species, we found high F_{ST} across these barriers,
122 exceeding the level of differentiation between the two species at a single location (Fig. 2B;
123 Supplementary Fig. 6B), indicating that ecological discontinuities may have a stronger impact on gene
124 flow than assortative mating in sympatric populations.

125 The movement of mosquitoes affects not only the spread of genetic variants in vector populations, but
126 also the spatial and temporal dynamics of malaria parasite transmission. Previous studies have
127 suggested that purposeful movement of individual *Anopheles* mosquitoes is limited to short-range
128 dispersal up to 5km^{52,53}; however, recent studies have provided evidence of long-distance seasonal
129 migration in *An. gambiae*¹⁴. If mosquitoes only travel short distances, we would expect to observe some
130 differentiation between mosquitoes sampled from different geographical locations. To complement
131 ADMIXTURE, PCA and F_{ST} results, we also studied the sharing of rare alleles (Fig. 2D), which should be
132 enriched for recent mutations and thus provide high resolution to detect subtle population structure. All
133 analyses provided evidence for differentiation between Uganda and *An. gambiae* populations to the
134 west, and between Guinea-Bissau and *An. coluzzii* from Burkina Faso (Fig. 2D; Supplementary Figs. 5, 6).
135 However, we found no evidence for differentiation between *An. gambiae* from Guinea and Burkina Faso
136 by any method. Some differentiation was detectable between *An. gambiae* from Burkina Faso and
137 Cameroon, but mosquitoes were sampled from multiple sites within Cameroon along an ecological cline
138 from savanna into rainforest, and there was evidence for some population structure and admixture
139 associated with these different ecosystems (Fig 2B; Supplementary Figs. 5A, 6A). Considering only the
140 Cameroon savanna site, differentiation between Cameroon and *An. gambiae* populations to the west
141 was extremely weak (Fig 2D; Supplementary Fig. 6B). These findings are consistent with substantial rates
142 of long-distance movement between savanna *An. gambiae* populations in West and Central Africa.

143 To examine gene flow between species in more detail, we analyzed a set of 506 SNPs previously found
144 to be highly differentiated between the two species in Mali¹⁸. These ancestry-informative markers
145 (AIMs) showed that a block of *An. gambiae* ancestry towards the centromere of chromosome arm 2L
146 has introgressed into *An. coluzzii* populations in both Burkina Faso and Angola (Supplementary Fig. 7).
147 This genomic region spans the *Vgsc* gene, where introgression of resistance mutations has previously
148 been reported in Ghana²⁴ and Mali²⁵, but this is the first evidence that introgressed mutations have
149 spread to *An. coluzzii* populations south of the Congo Basin rainforest. AIMs also showed that all
150 mosquitoes from Guinea-Bissau carried a mixture of *An. gambiae* and *An. coluzzii* alleles on all
151 chromosomes. These individuals were sampled from the coast, within a region of Far-West Africa that is
152 believed to be a zone of secondary contact between the two species, because mosquitoes have
153 frequently been found with a hybrid genotype at the species-diagnostic marker on the X chromosome,
154 and other genetic data have suggested extensive introgression^{20,22,54–56}. Our AIM results are consistent
155 with this interpretation; however, PCA and ADMIXTURE analyses of chromosome 3 showed no evidence
156 of recent admixture in Guinea-Bissau, rather grouping all individuals together in a single population
157 separate from other West African populations of either species (Supplementary Figs. 5A, 6A). These
158 results suggest a distinct demographic history for this population, and caution against the use of any
159 single marker to infer species ancestry or recent hybridization. This point is reinforced by the
160 observation that all mosquitoes sampled from coastal Kenya also carried a mixture of species alleles at
161 AIMs on all chromosome arms, except for a 4 Mbp region of chromosome X spanning the location of the
162 conventional diagnostic marker, where only *An. gambiae* alleles were present (Supplementary Fig. 7).
163 This mixed ancestry was unexpected, as sympatry between *An. gambiae* and *An. coluzzii* does not
164 extend east of the Rift Zone, where it is generally assumed that *An. gambiae*, *An. arabiensis* and *An.*
165 *merus* are the only representatives of the *gambiae* complex¹⁵. There are several hypotheses that could
166 explain our AIM results for Kenya, including recent or historical admixture with *An. coluzzii* populations,

167 introgression with other species, or retention of ancestral variation. Further analyses and population
168 sampling will be required to resolve these questions; however, our data clearly demonstrate that a
169 simple *gambiae/coluzzii* species dichotomy is not sufficient to capture the rich diversity and complex
170 histories of contemporary populations.

171 Variations in population size

172 Demographic events in the history of a population, including expansions or contractions in effective
173 population size (N_e), can be inferred from the genomes of extant individuals⁵⁷. For malaria vectors,
174 inferring changes in N_e has practical relevance, because it could provide a means to evaluate the impact
175 of vector control interventions. For each population, we computed summary statistics of genetic
176 diversity that are influenced by demographic history, including nucleotide diversity (π), site frequency
177 spectra (SFS) and decay of linkage disequilibrium (LD) (Fig. 3A). All populations north of the Congo Basin
178 rainforest and west of the Rift Zone had characteristics of large N_e and population expansion, with high
179 diversity ($\pi = 1.5\%$), an excess of rare variants (Tajima's $D < -1.5$) and extremely rapid decay of LD ($r^2 <$
180 0.01 within $< 1\text{ kbp}$). In Gabon and Angola, we found lower diversity, more extensive LD, and an SFS
181 closer to the null expectation under constant population size, indicating smaller N_e and different
182 demographic histories. In Kenya, we found the lowest level of diversity ($\pi = 0.9\%$), a strong deficit of rare
183 variants (Tajima's $D > 2$), and much longer LD ($r^2 > 0.01$ at 10 Mbp), suggesting a recent population
184 bottleneck.

185 We inferred the scale and timing of historical changes in N_e using two methods, Stairway Plot⁵⁸ and
186 ∂adi ⁵⁹, both using site frequency spectra but taking different modelling approaches. Stairway Plot
187 inferred a major expansion in all populations north of the Congo Basin rainforest and west of the Rift
188 Zone (Fig. 3B; Supplementary Fig. 8A). Three-epoch ∂adi models also inferred expansions in these
189 populations, with comparable magnitudes and timings (Supplementary Fig. 8B). Translating these results

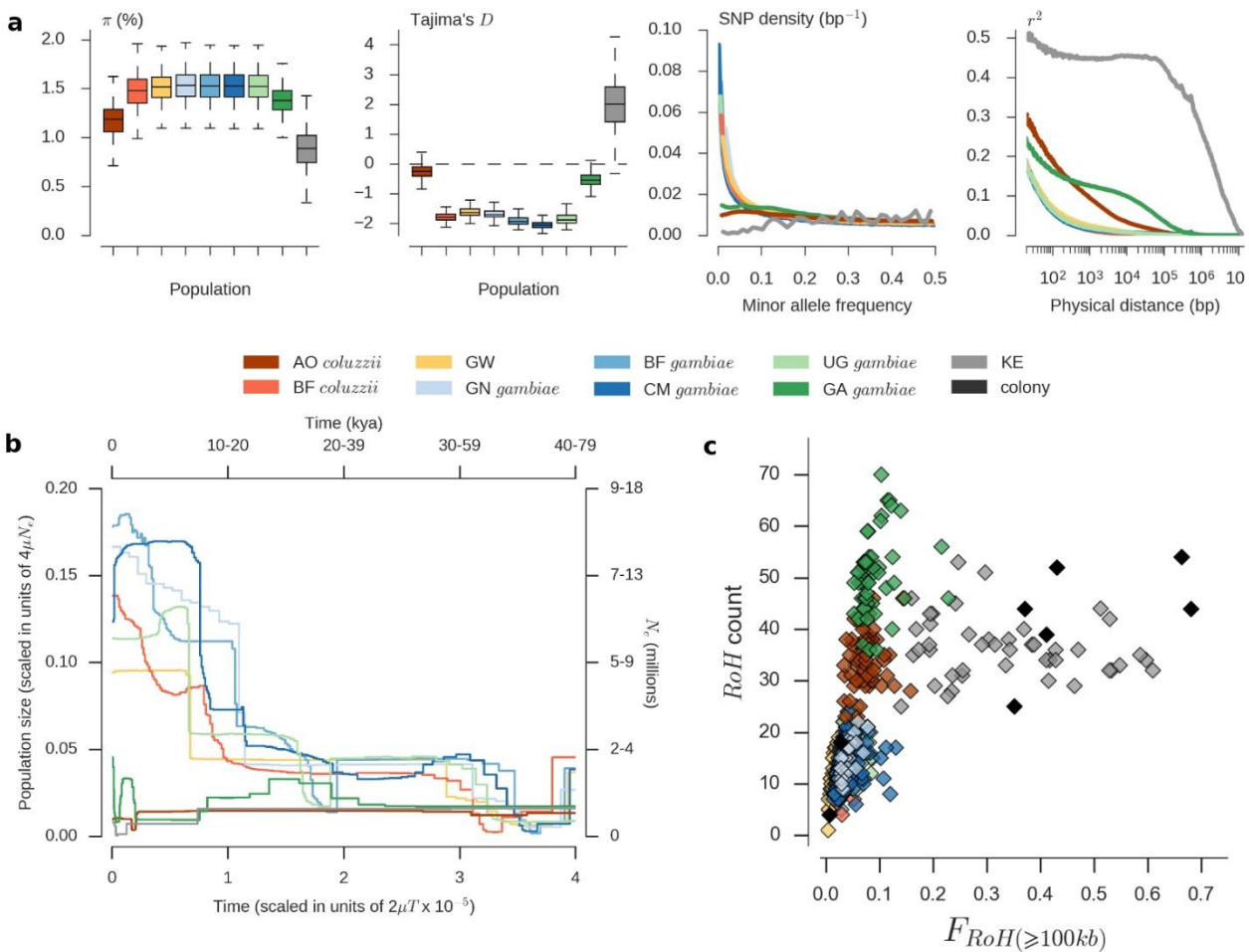


Figure 3. Genetic diversity and population size history. **a**, Statistics summarizing features of genetic diversity within each population. Nucleotide diversity (π) and Tajima's D are shown as the distribution of values calculated in non-overlapping 20kbp genomic windows. SNP density depicts the distribution of allele frequencies (site frequency spectrum) for each population, scaled such that a population with constant size over time is expected to have a constant SNP density over all allele frequencies. **b**, Stairway Plot of changes in population size over time, inferred from site frequency spectra. Absolute values of time and N_e are shown on alternative axes as a range of values, assuming lower and upper limits for the mutation rate as 2.8×10^{-9} and 5.5×10^{-9} respectively, and assuming $T=11$ generations per year. **c**, Runs of homozygosity in individual mosquitoes, highlighting evidence for recent inbreeding in Kenyan (grey) and colony (black) mosquitoes.

190 into absolute values for the timing and scale of expansion depends on the mutation rate, which has not
 191 been estimated in *Anopheles*. Estimates in *Drosophila*^{60,61} range from 2.8×10^{-9} to 5.5×10^{-9} , which would
 192 date the onset of a major expansion in the range 7,000 to 25,000 years ago (Fig. 3B). *An. gambiae* and
 193 *An. coluzzii* are both highly anthropophilic and so should have benefited from historical human
 194 population growth, particularly the expansion of agricultural Bantu-speaking groups originating from
 195 north of the Congo Basin beginning $\sim 5,000$ years ago⁶²⁻⁶⁵. The difference in timing suggests that either

196 the true mutation rate in *Anopheles* is higher than we have assumed, or that mosquito populations
197 benefited from some earlier human population growth or another factor. There have also been major
198 climatic changes since the last glacial maximum ~20,000 years ago, when overall environmental
199 conditions in Africa were much drier than present⁶⁶. If a general reduction in aridity was the major
200 driver, then we might expect to see evidence for expansion in all mosquito populations sampled.
201 However, we inferred different demographic histories in Angola, Gabon and Kenya, although more
202 recent N_e fluctuations may be obscuring earlier events in these populations, particularly in Gabon and
203 Kenya (Fig. 3B; Supplementary Fig. 8).

204 In Kenya in 2006, free mass distribution of ITNs was carried out in multiple districts, resulting in a rapid
205 increase in ITN coverage, from less than 10% in 2004 to over 60% by the beginning of 2007⁶⁷.
206 Mosquitoes for this study were sampled from Kilifi County in 2012, and therefore originate from
207 populations experiencing sustained ITN pressure for several years. To investigate evidence for a very
208 recent bottleneck in this population, we analyzed runs of homozygosity (ROH). Kenyan mosquitoes had
209 between 10-60% of their genome within a long ROH, a level not seen in any other population (Fig. 3C).
210 This level of homozygosity is comparable to that found in isolated human populations⁶⁸ and domestic
211 animal breeds⁶⁹ due to recent inbreeding. We also observed similar ROH in mosquitoes originating from
212 lab colonies, which are typically maintained in cages of at most a few hundred individuals, and thus
213 where inbreeding is inevitable (Fig. 3C). Genetic signatures of recent inbreeding have previously been
214 observed in a mosquito population from Burkina Faso⁷⁰ and in a separate study of mosquitoes collected
215 from Kilifi in 2010⁷¹. However, there remains uncertainty as to whether ITN scale-up is the root cause of
216 mosquito population decline in Kilifi⁷¹, particularly as other studies have found evidence for lower N_e ⁴⁸
217 and changes in species abundance⁷² in the region pre-dating high levels of ITN coverage. Furthermore,
218 while ITNs have been effective in Kilifi, a substantial reduction in malaria prevalence had occurred prior
219 to free ITN distribution⁷³, thus multiple factors may be affecting vector and parasite populations in this

220 region. Sequencing mosquitoes and parasites before, during and after interventions, and across a range
221 of ecological and epidemiological settings, could help to resolve these questions, providing valuable
222 information about the impact and efficacy of different control strategies.

223 Evolution of insecticide resistance

224 Insecticide resistance is a polygenic trait with a broad phenotypic range, and several genes have
225 previously been associated with resistance in *Anopheles*, including genes encoding insecticide binding
226 targets and genes involved in insecticide metabolism³. It is not yet clear which of these genes, if any, are
227 responsible for epidemiologically relevant levels of resistance in the field. However, mutations that
228 confer an advantage under strong pressure from insecticide use will be positively selected, and so
229 evidence of recent selection in natural populations can help to identify and prioritize resistance genes
230 for further study. We used metrics of haplotype diversity⁷⁴ (H12) and haplotype homozygosity⁷⁵ (XP-
231 EHH) to scan the genome for genes with evidence of recent selection. Both metrics revealed strong
232 signals of selection in multiple populations at several genome locations containing genes associated with
233 insecticide resistance (Fig. 4; Supplementary Fig. 9). These included *Vgsc*, confirming evidence for
234 selection from population structure analyses described above; *Gste*, a cluster of glutathione S-
235 transferase genes including *Gste2*, previously implicated in metabolic resistance to DDT and
236 pyrethroids^{76,77}; and *Cyp6p*, a cluster of genes encoding cytochrome P450 enzymes, including *Cyp6p3*
237 which is upregulated in permethrin and bendiocarb resistant mosquitoes^{78,79}.

238 Mutations in *An. gambiae Vgsc* codon 995 (orthologous to *Musca domestica Vgsc* codon 1014), known
239 as “*kdr*” due to their knock-down resistance phenotype, reduce susceptibility to DDT and pyrethroids by
240 altering binding-site conformation⁴⁶. We found the Leucine→Phenylalanine (L995F) *kdr* mutation at high
241 frequency in West and Central Africa (Guinea 100%; Burkina Faso 93%; Cameroon 53%; Gabon 36%;

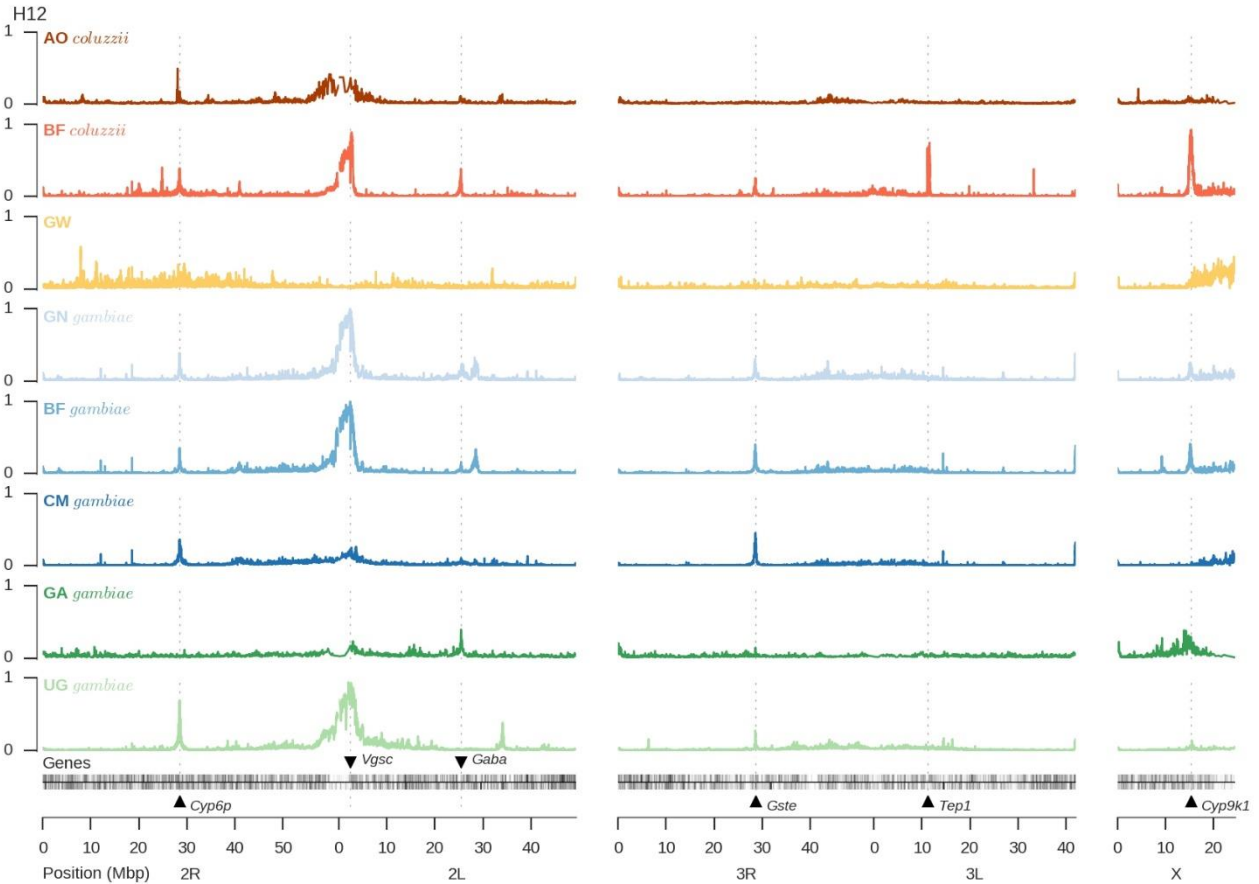


Figure 4. Genome scans for signatures of recent selection. Each track plots the H12 statistic in non-overlapping windows over the genome. A value of 1 indicates low haplotype diversity within a window, expected if one or two haplotypes have risen to high frequency due to recent selection. A value of 0 indicates high haplotype diversity, expected in neutral regions. Kenya is not shown because the high genome-wide levels of homozygosity mean reduced power to detect evidence of recent selection in specific genome regions.

242 Angola 86%). A second *kdr* allele, the Leucine→Serine (L995S) mutation, was present in Central and East
243 Africa (Cameroon 15%; Gabon 65%; Uganda 100%; Kenya 76%). To investigate the origins and
244 movements of these two distinct *kdr* mutations, we analyzed the genetic backgrounds on which they
245 were carried, using information from all 1,718 biallelic SNPs found across both coding and non-coding
246 regions of the *Vgsc* gene (Fig. 5). The L995F mutation occurred in five distinct haplotype clusters (labeled
247 F1-F5 in Fig. 5), while the L995S mutation was found in a further 5 haplotype clusters (labeled S1-S5 in
248 Fig. 5), indicating that the number of independent origins for each of these mutations is higher than
249 previously estimated^{80–82}. Several *kdr* haplotypes have also spread between populations, despite

250 considerable geographic distance or ecological separation. For example, haplotype F1 is present in both
251 species and in 4 countries spanning the Congo Basin rainforest, and is the same haplotype previously
252 found to be introgressed from *An. gambiae* into *An. coluzzii* in Ghana²⁴, indicating strong selection
253 across a variety of ecological settings. Additionally, three *kdr* haplotypes (F4, F5, S2) were found in both
254 Cameroon and Gabon, providing multiple examples of recent adaptive gene flow between these two
255 otherwise highly differentiated populations. Finally, the S3 haplotype was found in both Uganda and
256 Kenya, showing that adaptive alleles can even cross the Rift Zone. While these remarkable patterns of
257 evolution and adaptive gene flow were primarily driven by the two *kdr* mutations, we found 16 other
258 non-synonymous mutations within *Vgsc* at a frequency above 1% (Fig. 5), of which 13 occurred
259 exclusively on haplotypes carrying the L995F *kdr* mutation, suggesting secondary selection acting on
260 mutations that enhance or compensate for the primary *kdr* phenotype.

261 Metabolic resistance is of particular concern as it has been implicated in extreme resistance phenotypes
262 observed in some *Anopheles* populations⁷⁹. At both *Gste* and *Cyp6p* we found evidence that resistance
263 has emerged multiple times, and is also spreading between species and over considerable distances. At
264 the *Gste* locus we found at least four distinct haplotypes under selection (Supplementary Fig. 10A). One
265 of these haplotypes carried the *Gste2*-I114T mutation which enhances DDT metabolism^{77,83}, though the
266 other three haplotypes did not carry any known resistance mutations. At the *Cyp6p* locus we found at
267 least eight distinct haplotypes under selection (Supplementary Fig. 10B). Clearly there is much to learn
268 regarding the molecular basis of metabolic resistance, and our SNP data can be used to identify
269 candidate resistance mutations. For example, at both loci we found multiple non-synonymous SNPs that
270 were strongly associated with haplotypes under selection (Supplementary Fig. 10). These data provide a
271 starting point for new studies to characterize resistance phenotypes, and to develop improved tools for
272 monitoring and responding to the emergence and spread of resistance in natural populations.

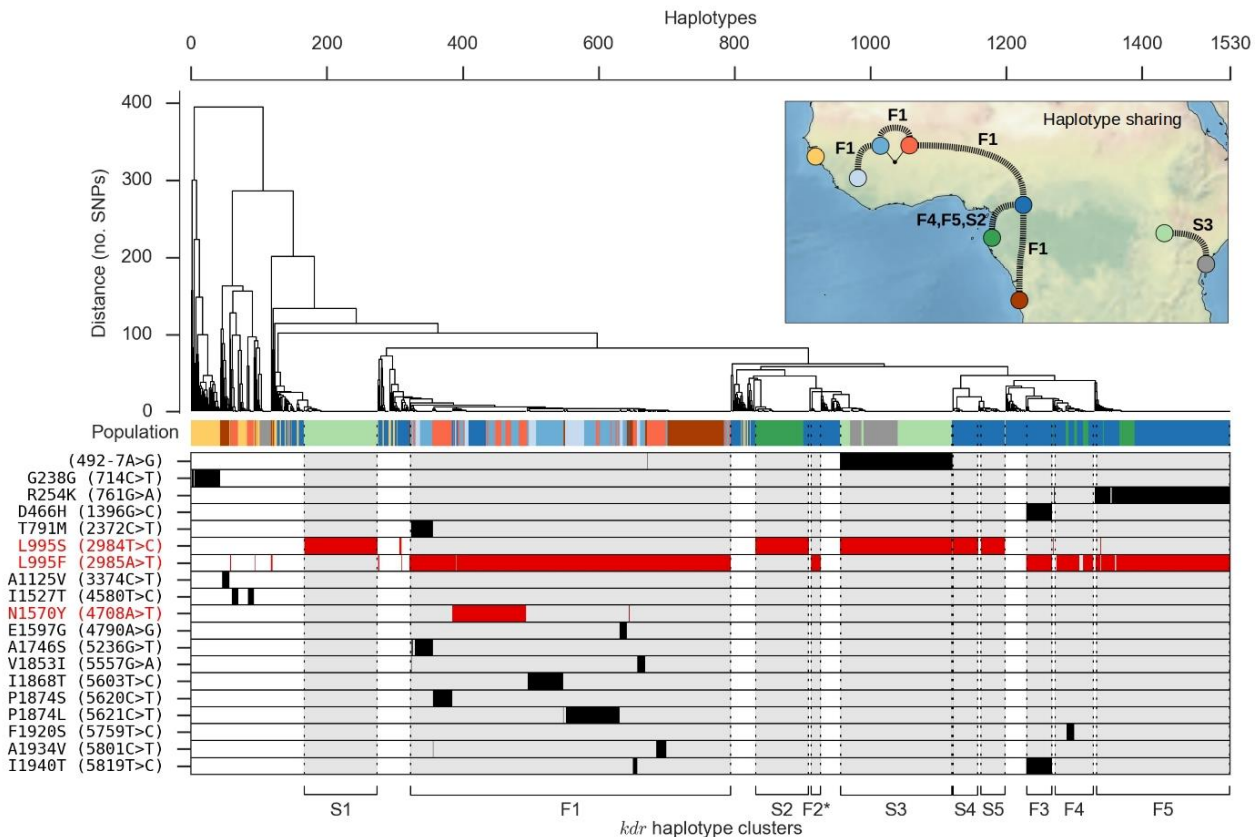


Figure 5. Haplotype structure at the *Vgsc* gene. The upper panel shows a dendrogram obtained by hierarchical clustering of haplotypes from wild-caught individuals. The colour bar immediately below shows the population of origin for each haplotype. Inset map depicts haplotypes shared between populations. The lower panel shows alleles carried by each haplotype at 19 SNPs with allele frequency > 1% that either change the amino acid sequence or occur within a splice region, and therefore may affect protein function (white = reference allele; black = alternate allele; red = previously known resistance-conferring allele). At the lower margin, we label 10 haplotype clusters carrying a *kdr* mutation (either L995F or L995S).

273 Discussion

274 In this first phase of the Ag1000G project we have focused on nucleotide variation, revealing an
 275 extraordinary reservoir of natural genetic diversity in mosquito populations. Nucleotide diversity is 1.5%
 276 in most populations, twice that reported for African populations of *Drosophila melanogaster*^{37,84} and ten
 277 times greater than human populations³⁰, sustained by a network of large and highly interconnected
 278 populations. The genomes that we have sequenced convey a rich mosaic of different ancestries, shaped
 279 by geography, ecology, speciation, migration, selection, recombination and chromosomal inversions,
 280 with different forces predominating in different genomic regions. Mosquito populations in different

281 parts of Africa have experienced major demographic changes, including expansions and contractions in
282 size, influenced at least in part by major events in the history of our own species. The introduction of
283 insecticides has led to intense selection pressure, repeatedly driving resistance mutations to high
284 frequency and demonstrating the potential for adaptive gene flow across the entire continent. The data
285 we have generated provide a resource for studying and responding to the ongoing evolution of malaria
286 vector populations. To facilitate access to this resource we have developed a novel web application[‡] that
287 enables visual exploration of genomic data on populations and individual mosquitoes from the scale of a
288 whole chromosome down to individual nucleotides. Future project phases will increase both the
289 geographical and taxonomic representation of mosquito genomes sequenced, and will explore other
290 forms of genetic variation, including small insertion/deletion polymorphisms and large structural
291 variation. We will also continue to study fundamental population-genetic processes, including mutation,
292 recombination, natural selection, and the fine structure and history of gene flow between populations.

293 In 1899 Ronald Ross proposed that malaria could be controlled by destroying breeding sites of the
294 mosquitoes that transmit the disease⁸⁵. *An. gambiae*, identified in the same year by Ross as a vector of
295 malaria in Africa⁸⁶, has proved resilient to a century of attempts to repress it. The vector control
296 armamentarium needs to be expanded, not only with new classes of insecticide and novel genetic
297 control strategies, but also with more effective tools for gathering intelligence, to enable those
298 responsible for planning and executing interventions to stay ahead of the mosquito's remarkable
299 capacity for evolutionary adaptation. There remain major knowledge gaps, e.g., concerning the rate and
300 range of long-distance migration, which are fundamental to understanding both malaria transmission
301 and the spread of insecticide resistance, and which will require detailed spatiotemporal analysis of
302 mosquito population structure. Most importantly, it is essential to start collecting population genomic
303 data prospectively as an integral part of major vector control interventions, to identify which strategies

[‡] <http://www.malariagen.net/apps/ag1000g>

304 are most likely to cause increased resistance, or what it takes to cause a population crash of the
305 magnitude observed in our Kenyan data. By treating each major intervention as an experiment, and by
306 analyzing its impact on mosquito populations, we can aim to improve the efficacy and sustainability of
307 future interventions, while at the same time learning about basic processes of ecology and evolution.

308 **Methods**

309 Methods are described in Supplementary Text.

310 **Data availability**

311 All sequence reads from the Ag1000G project are available from the European Nucleotide Archive (ENA -
312 <http://www.ebi.ac.uk/ena>) under study PRJEB1670. Submission of sequence read alignments and
313 variant calls from Ag1000G phase 1 is in progress under ENA study PRJEB18691. Variant and haplotype
314 calls and associated data from Ag1000G phase 1 can be explored via an interactive web application or
315 downloaded via the MalariaGEN website (<https://www.malariagen.net/projects/ag1000g#data>).

316 **Acknowledgments**

317 This work was supported by the Wellcome Trust (090770/Z/09/Z; 090532/Z/09/Z; 098051) and Medical
318 Research Council UK and the Department for International Development (DFID) (MR/M006212/1). The
319 authors would like to thank the staff of Wellcome Trust Sanger Institute Sample Logistics, Sequencing
320 and Informatics facilities for their contributions. SO'L and AB were supported by a grant from the
321 Foundation for the National Institutes of Health through the Vector-Based Control of Transmission:
322 Discovery Research (VCTR) program of the Grand Challenges in Global Health initiative of the Bill &
323 Melinda Gates Foundation.

324 *The Anopheles gambiae* 1000 Genomes Consortium

325 **Corresponding authors.** Alistair Miles^{1,2}, Mara K. N. Lawniczak¹, Martin Donnelly^{3,1}, Dominic

326 Kwiatkowski^{1,2}.

327 **Data analysis group.** Alistair Miles^{1,2} (project lead), Nicholas J. Harding², Giordano Bottà^{4,2}, Chris S.

328 Clarkson¹, Tiago Antão⁵, Krzysztof Kozak¹, Daniel R. Schrider⁶, Andrew D. Kern⁶, Seth Redmond⁷, Igor

329 Sharakhov^{8,9}, Richard D. Pearson^{1,2}, Christina Bergey¹⁰, Michael C. Fontaine¹¹, Martin Donnelly^{3,1}, Mara K.

330 N. Lawniczak¹, Dominic Kwiatkowski^{1,2} (chair).

331 **Partner working group.** Martin Donnelly^{3,1} (chair), Diego Ayala^{12,13}, Nora J. Besansky¹⁰, Austin Burt¹⁴,

332 Beniamino Caputo⁴, Alessandra della Torre⁴, Michael C. Fontaine¹¹, H. Charles J. Godfray¹⁵, Matthew W.

333 Hahn¹⁶, Andrew D. Kern⁶, Dominic Kwiatkowski^{1,2}, Mara K. N. Lawniczak¹, Janet Midega¹⁷, Daniel E.

¹ Malaria Programme, Wellcome Trust Sanger Institute, Hinxton, Cambridge CB10 1SA, UK

² MRC Centre for Genomics and Global Health, University of Oxford, Oxford OX3 7BN, UK

³ Department of Vector Biology, Liverpool School of Tropical Medicine, Pembroke Place, Liverpool L3 5QA, UK

⁴ Istituto Pasteur Italia – Fondazione Cenci Bolognetti, Dipartimento di Sanità Pubblica e Malattie Infettive, Università di Roma SAPIENZA, Rome, Italy

⁵ University of Montana, Missoula, MT 59812, USA

⁶ Department of Genetics, Rutgers University, 604 Alison Road, Piscataway, NJ 08854, USA

⁷ Genome Sequencing and Analysis Program, Broad Institute, 415 Main Street, Cambridge, MA 02142, USA

⁸ Department of Entomology, Virginia Tech, Blacksburg, VA 24061, USA

⁹ Laboratory of Ecology, Genetics and Environmental Protection, Tomsk State University, Tomsk 634050, Russia

¹⁰ Eck Institute for Global Health, Department of Biological Sciences, University of Notre Dame, IN 46556, USA

¹¹ Groningen Institute for Evolutionary Life Sciences (GELIFES), Nijenborgh 7, 9747 AG Groningen, The Netherlands

¹² Unité d'Ecologie des Systèmes Vectoriels, Centre International de Recherches Médicales de Franceville, Franceville, Gabon

¹³ Institut de Recherche pour le Développement (IRD), UMR MIVEGEC (UM1, UM2, CNRS 5290, IRD 224), Montpellier, France

¹⁴ Department of Life Sciences, Imperial College, Silwood Park, Ascot, Berkshire SL5 7PY, UK

¹⁵ Department of Zoology, University of Oxford, The Tinbergen Building, South Parks Road, Oxford OX1 3PS, UK

¹⁶ Department of Biology and School of Informatics and Computing, Indiana University, Bloomington, IN 47405, USA

¹⁷ KEMRI-Wellcome Trust Research Programme, PO Box 230, Bofa Road, Kilifi, Kenya

- 334 Neafsey⁷, Samantha O’Loughlin¹⁴, João Pinto¹⁸, Michelle Riehle¹⁹, Igor Sharakhov^{8,9}, Kenneth D.
335 Vernick²⁰, David Weetman³, Craig Wilding²¹, Bradley White²².
- 336 **Sample collections. Angola:** Arlete D. Troco²³, João Pinto¹⁸; **Burkina Faso:** Abdoulaye Diabaté²⁴,
337 Samantha O’Loughlin¹⁴, Austin Burt¹⁴; **Cameroon:** Carlo Costantini^{13,25}, Kyanne R. Rohatgi¹⁰, Nora J.
338 Besansky¹⁰; **Gabon:** Nohal Elissa¹², João Pinto¹⁸; **Guinea:** Boubacar Coulibaly²⁶, Michelle Riehle¹⁹,
339 Kenneth D. Vernick²⁰; **Guinea-Bissau:** João Pinto¹⁸, João Dinis²⁷; **Kenya:** Janet Midega¹⁷, Charles Mbogo¹⁷,
340 Philip Bejon¹⁷; **Uganda:** Craig Wilding²¹, David Weetman³, Henry Mawejeje²⁸, Martin Donnelly^{3,1}; **Crosses:**
341 David Weetman³, Craig Wilding²¹, Martin Donnelly^{3,1}.
- 342 **Sequencing and data production.** Jim Stalker¹, Kirk Rockett², Eleanor Drury¹, Daniel Mead¹, Anna
343 Jeffreys², Christina Hubbart², Kate Rowlands², Alison Isaacs³, Dushyanth Jyothi¹, Cinzia Malangone¹.
- 344 **Web application development.** Paul Vauterin², Ben Jeffrey², Ian Wright², Lee Hart², Krzysztof
345 Kluczyński².
- 346 **Project coordination.** Victoria Cornelius², Bronwyn MacInnis²⁹, Christa Henrichs², Rachel
347 Giacomantonio¹, Dominic Kwiatkowski^{1,2}.

¹⁸ Global Health and Tropical Medicine, GHTM, Instituto de Higiene e Medicina Tropical, IHMT, Universidade Nova de Lisboa, UNL, Rua da Junqueira 100, 1349-008 Lisbon, Portugal

¹⁹ Department of Microbiology and Immunology, Microbial and Plant Genomics Institute, University of Minnesota, St. Paul, MN 55108

²⁰ Unit for Genetics and Genomics of Insect Vectors, Institut Pasteur, Paris, France

²¹ School of Natural Sciences and Psychology, Liverpool John Moores University, Liverpool L3 3AF, UK

²² Department of Entomology, University of California, Riverside, CA, USA

²³ Programa Nacional de Controle da Malária, Direção Nacional de Saúde Pública, Ministério da Saúde, Luanda, Angola

²⁴ Institut de Recherche en Sciences de la Santé (IRSS), Bobo Dioulasso, Burkina Faso

²⁵ Laboratoire de Recherche sur le Paludisme, Organisation de Coordination pour la lutte contre les Endémies en Afrique Centrale (OCEAC), Yaoundé, Cameroon

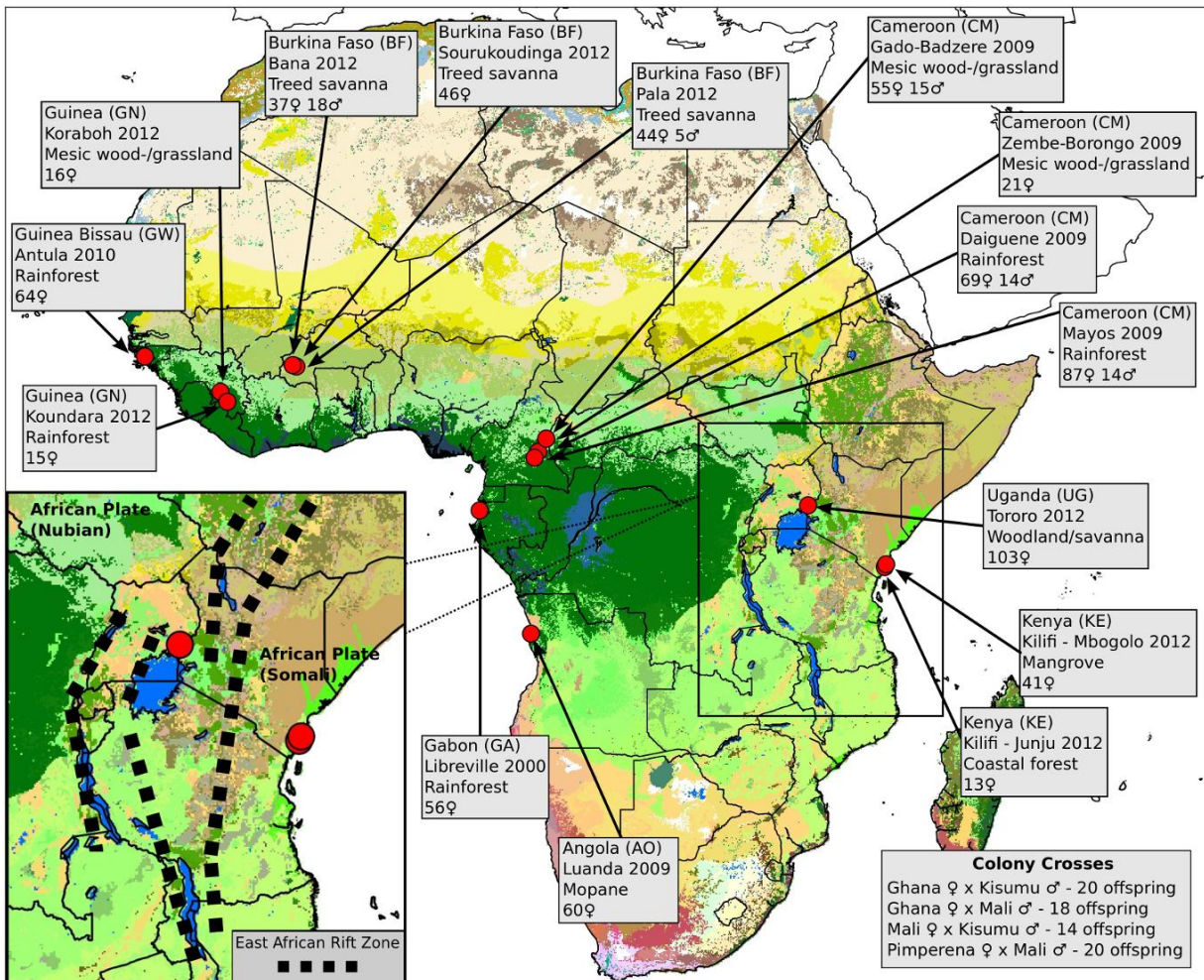
²⁶ Malaria Research and Training Centre, Faculty of Medicine and Dentistry, University of Mali

²⁷ Instituto Nacional de Saúde Pública, Ministério da Saúde Pública, Bissau, Guiné-Bissau

²⁸ Infectious Diseases Research Collaboration, 2C Nakasero Hill Road, P.O. Box 7475, Kampala, Uganda

²⁹ The Broad Institute of Massachusetts Institute of Technology and Harvard, 415 Main Street, Cambridge, MA 02142, USA

348 **Supplementary figures**

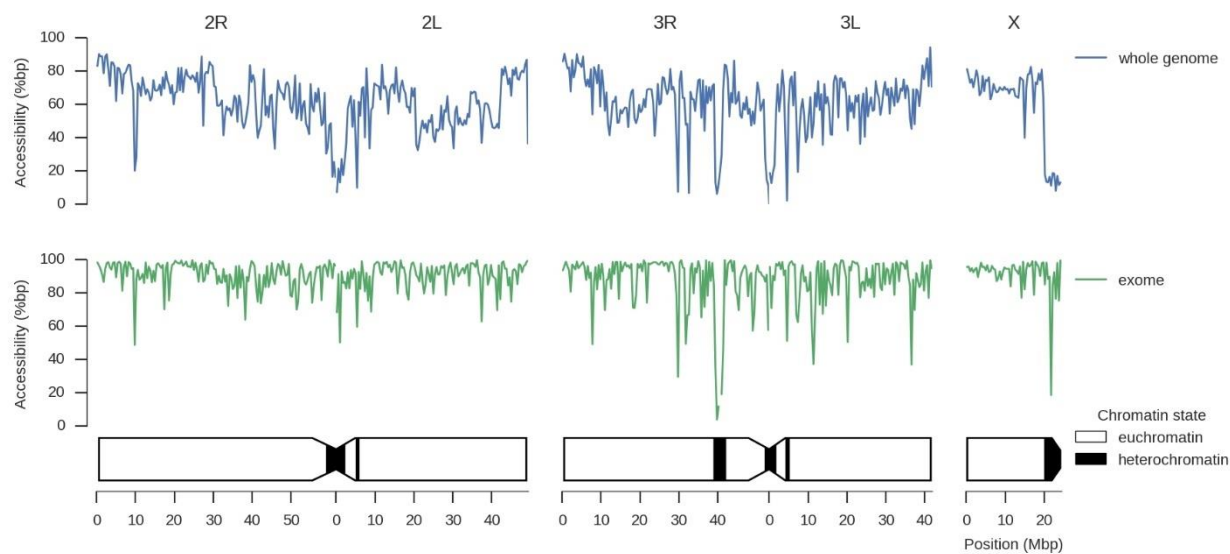


Supplementary Figure 1. Overview of population sampling. Red circles show sampling locations for wild-caught mosquitoes; black outlines show country borders. Colours in the map represent ecosystem classes; dark green represents forest ecosystems, see (87) Fig. 9 for a complete colour legend. The Congo Basin tropical rainforest is the large region of dark green in Central Africa, spanning parts of Cameroon, Equatorial Guinea, Gabon, Central African Republic, Republic of Congo and Democratic Republic of Congo. Sampling details for each site are shown in light grey boxes, including country (two-letter country code), name of sampling site, year of collection, predominant ecosystem classification⁸⁷ for the local region, and number and sex of individuals sequenced. Further details of sampling locations and methods are provided in Supplementary Text. For colony crosses, the direction of cross (colony of origin of mother and father) and number of offspring is shown. The inset map depicts geological fault lines in the East African Rift Zone*.

349

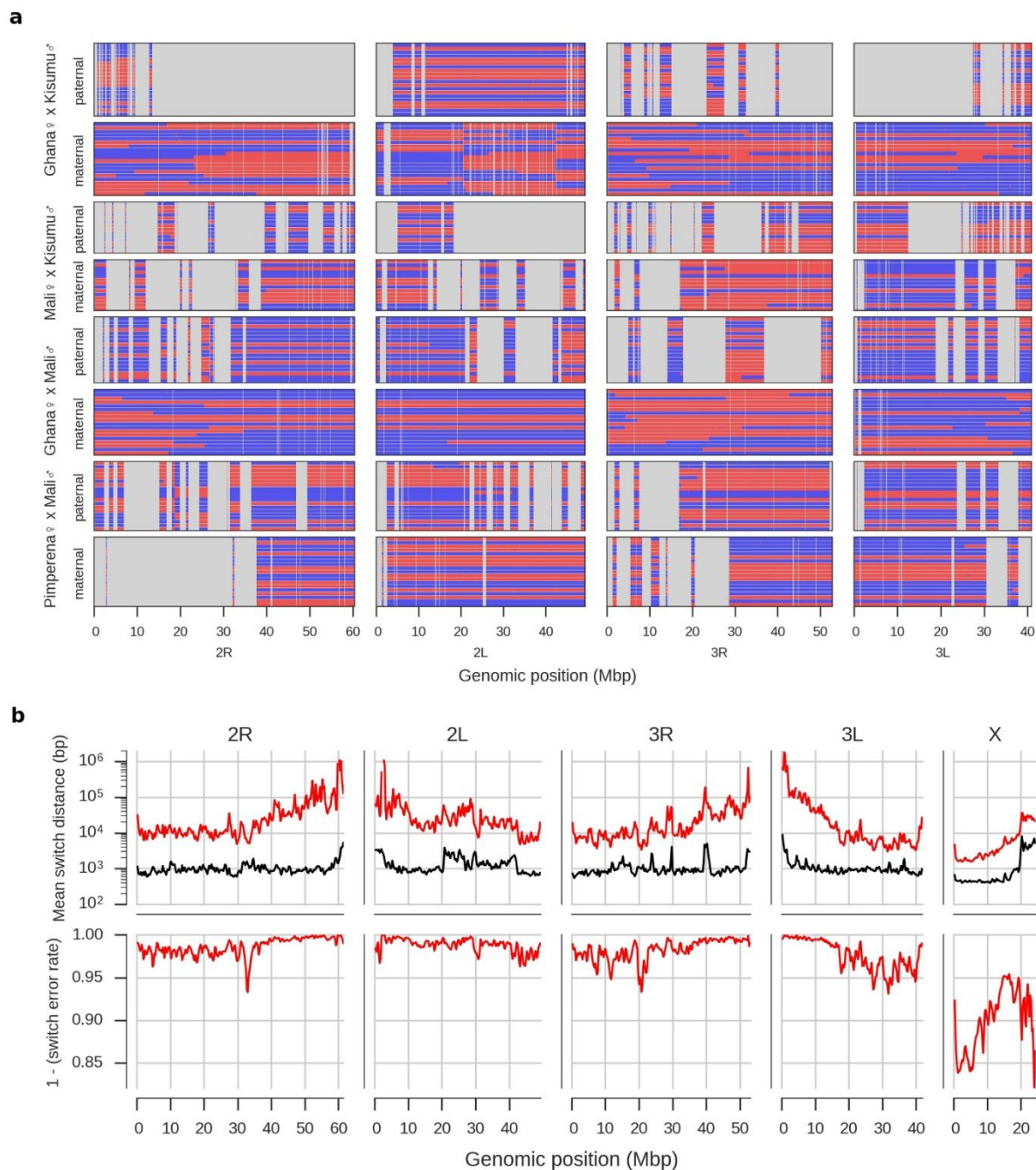
350

* http://pubs.usgs.gov/publications/text/East_Africa.html

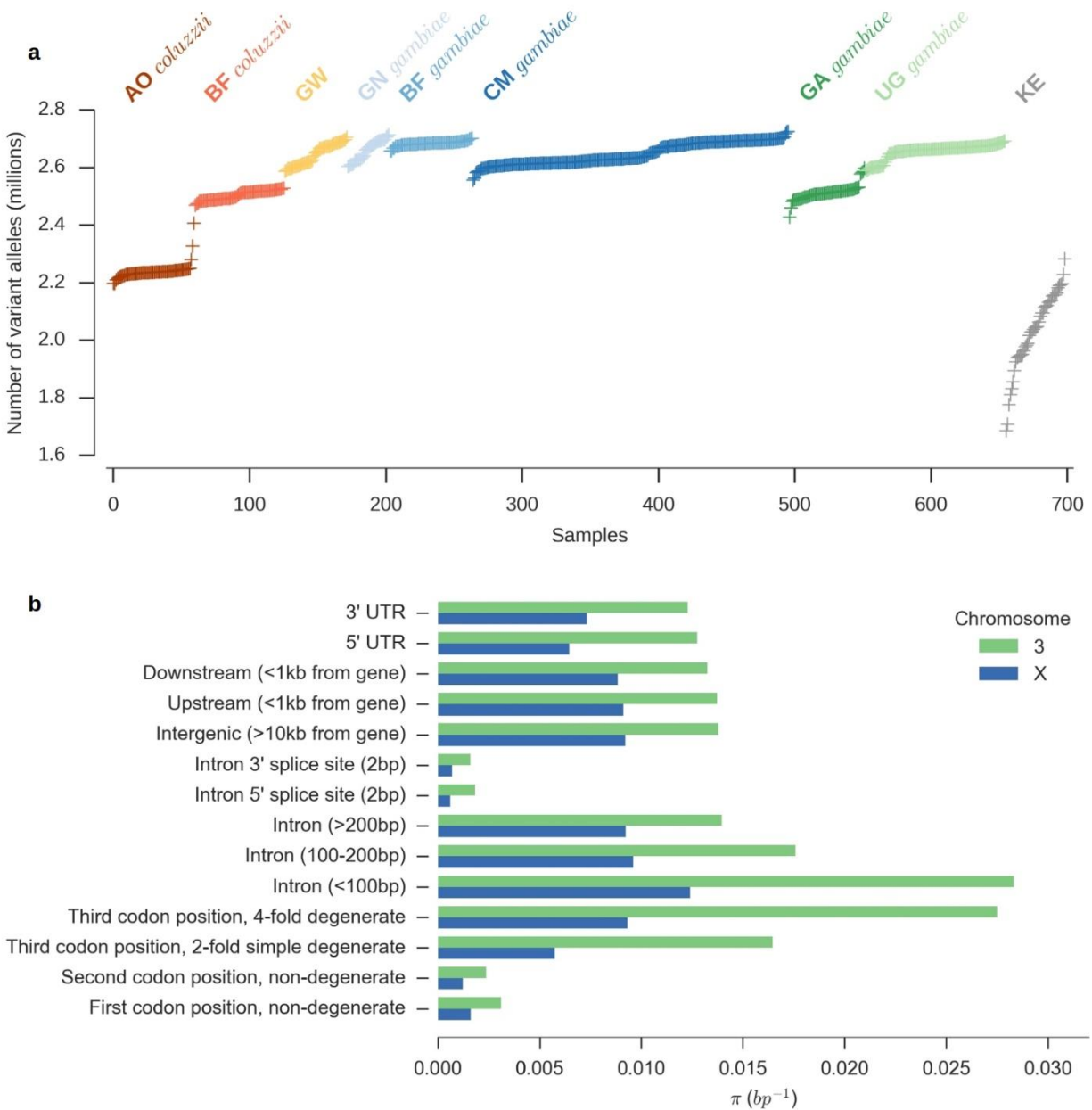


351

352



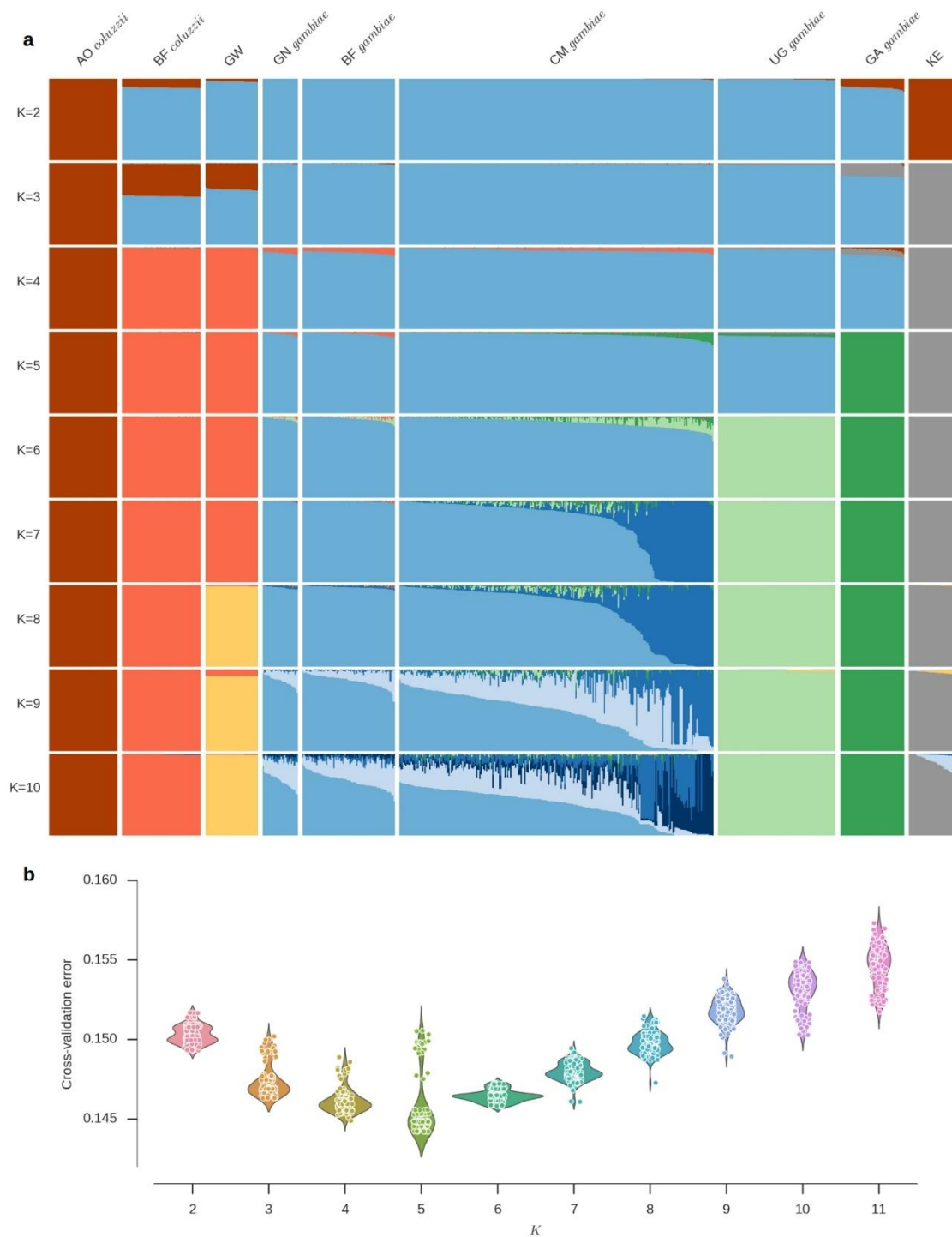
Supplementary Figure 3. Haplotype validation. **a**, Haplotypes inferred in the crosses. Each panel shows either maternal or paternal haplotypes from a single cross. Each row within a panel represents a single progeny haplotype. Haplotypes are coloured by parental inheritance (blue = allele from parent's first chromosome, red = allele from parent's second chromosome). Switches between colours along a haplotype indicate putative recombination events. Regions that were within a run of homozygosity in the parent and thus not informative for haplotype validation are masked in grey. **b**, Error rate estimates for haplotypes inferred in wild-caught individuals. Upper plots show estimates for the mean switch distance (red line) in windows over the genome, compared to the mean switch distance if heterozygotes were phased randomly (black line). Lower plots show the switch error rate, which estimates the probability of a switch error occurring between two adjacent heterozygous genotype calls.



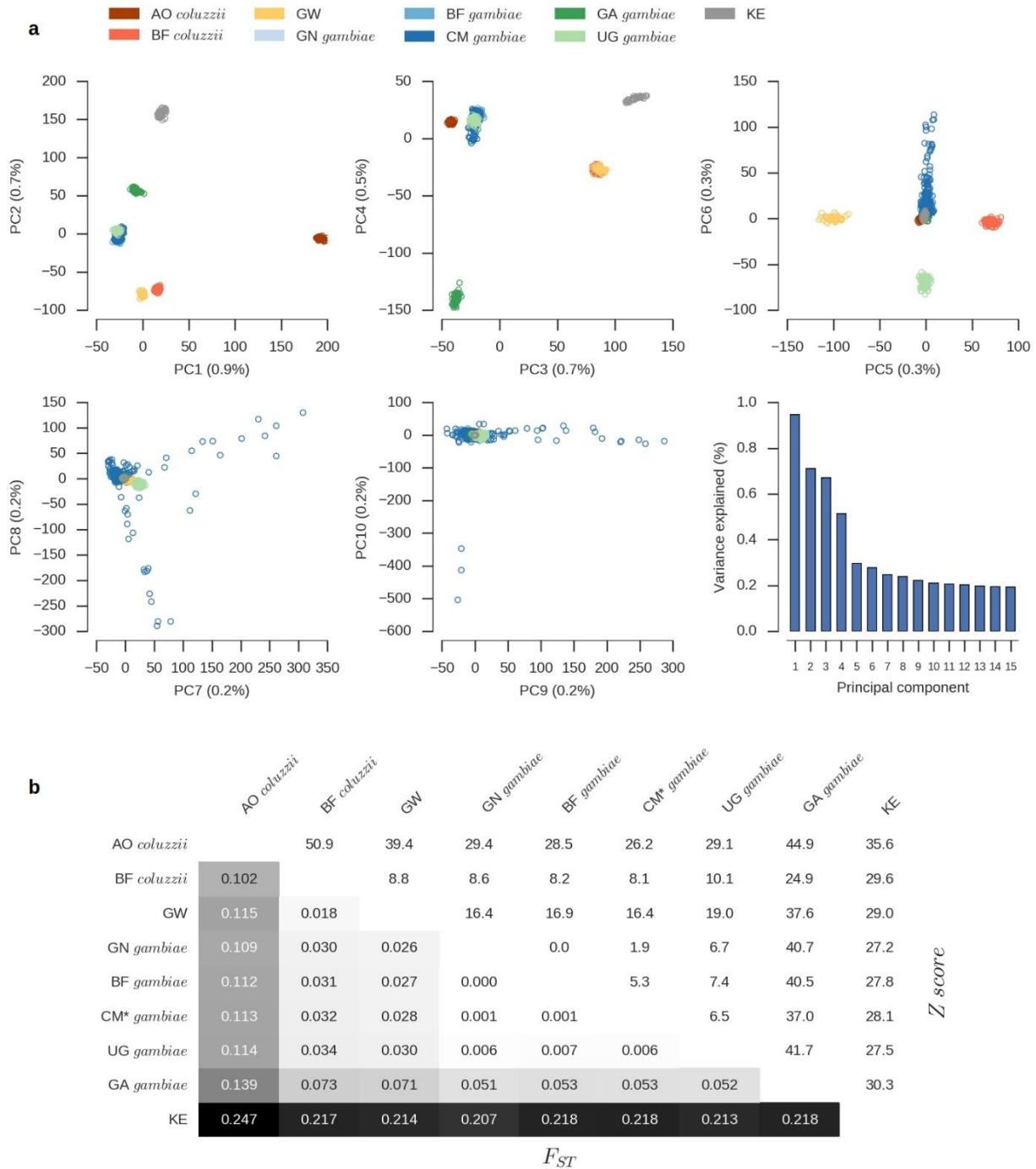
Supplementary Figure 4. Variant discovery and nucleotide diversity. **a**, Total number of variant alleles discovered per individual mosquito sequenced. Only females are plotted. **b**, Average nucleotide diversity (π) in relation to gene architecture.

353

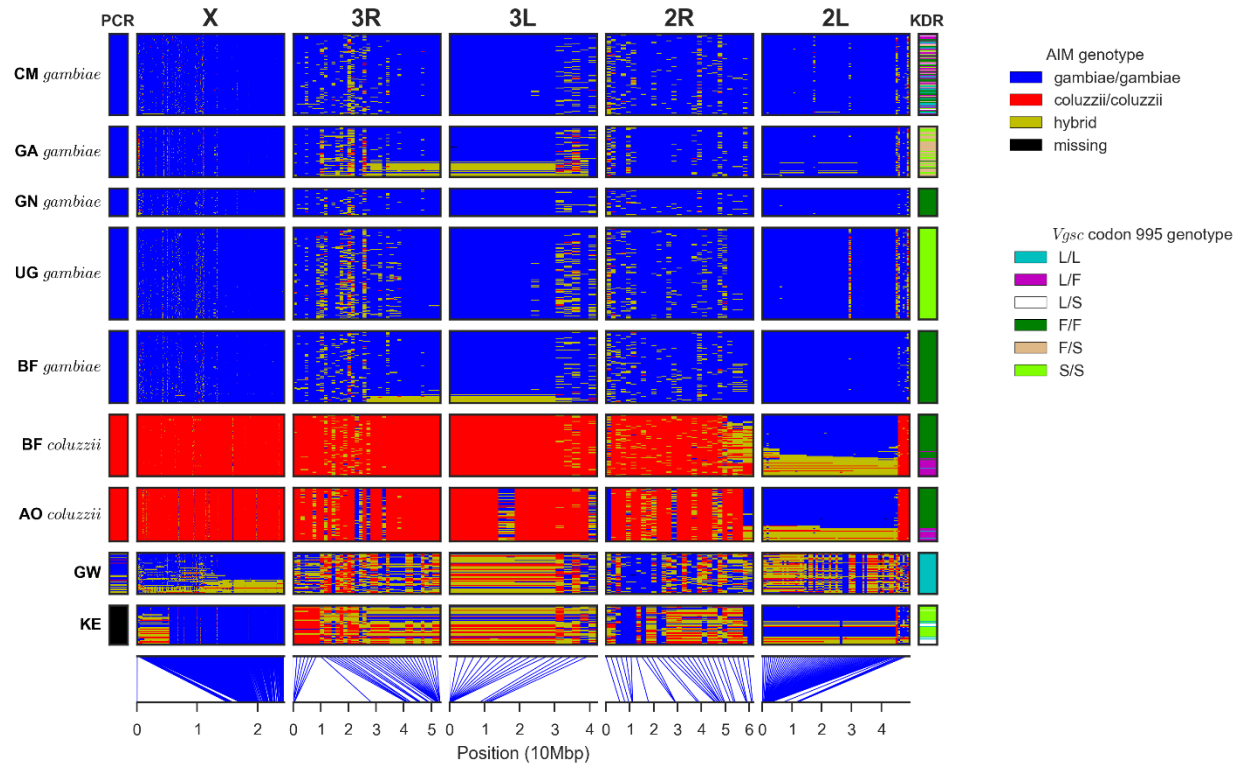
354



Supplementary Figure 5. ADMIXTURE analysis. **a**, Ancestry proportions within individual mosquitoes for ADMIXTURE models from $K=2$ to $K=10$ ancestral populations. Each vertical bar represents the proportion of ancestry within a single individual, with colours corresponding to ancestral populations. These data are the average of the major q -matrix clusters derived by CLUMPAK analysis. **b**, Violin plot of cross-validation error for each of 100 replicates for each K values.



Supplementary Figure 6. Population structure and allele frequency differentiation. **a**, Principal components analysis of the 765 wild-caught mosquitoes, showing the first 10 components of genetic variation. The final panel shows the variance explained by each component. **b**, Average allele frequency differentiation (F_{ST}) between pairs of populations. The lower left triangle shows average F_{ST} between each population pair. The upper right triangle shows the Z score for each F_{ST} value estimated via a block-jackknife procedure.



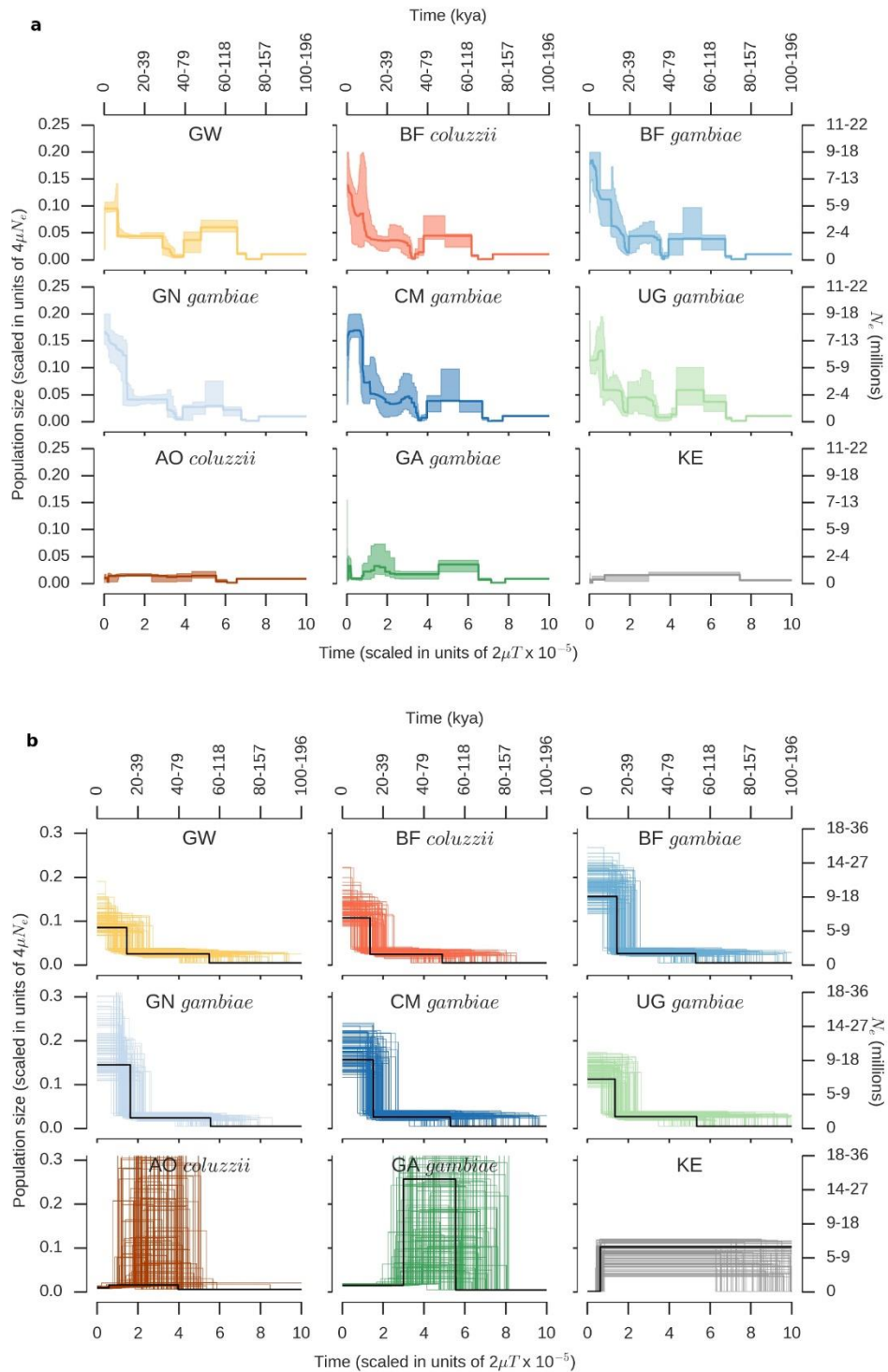
Supplementary Figure 7. Ancestry informative markers (AIMs). Rows represent individual mosquitoes (grouped by population) and columns represent SNPs (grouped by chromosome arm). Colours represent genotype. The column at the far left shows the species assignment according to the conventional molecular test based on a single marker on the X chromosome, which was performed for all individuals except Kenya (KE). The column at the far right shows the genotype for *kdr* mutations in *Vgsc* codon 995. Lines at the lower edge show the physical locations of the AIM SNPs.

357

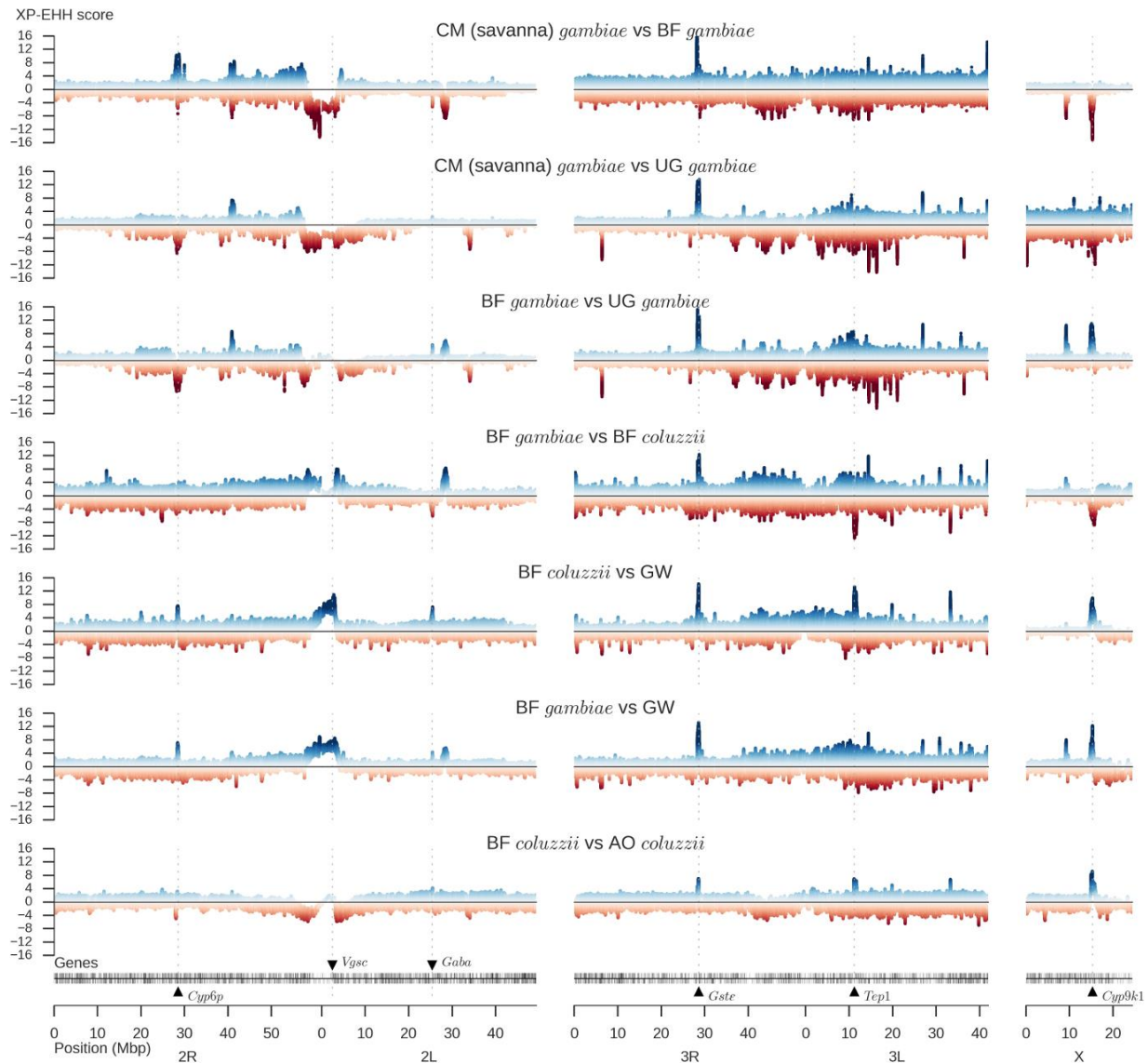
358

359

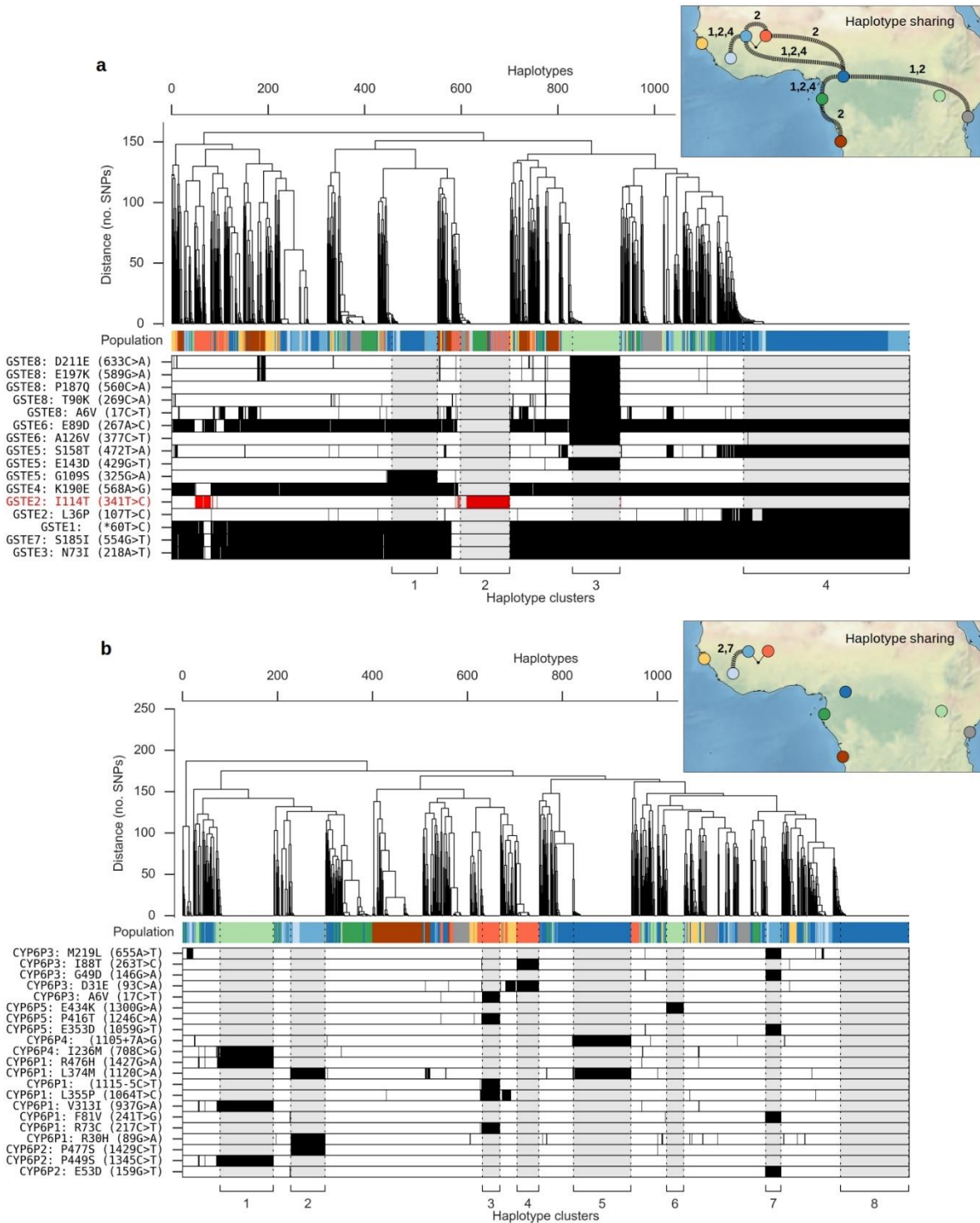
360



Supplementary Figure 8. Inferred population size histories. **a**, Stairway Plot inferred histories for each population. The shaded area shows the 95% confidence interval from 199 bootstrap replicates. **b**, Inferred histories from *dad*i three epoch models. Black line shows the history with the highest likelihood found by optimization; coloured lines show 100 histories with the highest likelihoods from even sampling of the model parameter space (Supplementary Text). Absolute time and N_e are shown as a range assuming 11 generations per year and a mutation rate of between 2.8×10^{-9} and 5.5×10^{-9} .



Supplementary Figure 9. Cross-population genome scans for signatures of recent selection. For each population comparison (e.g., BF *gambiae* versus BF *coluzzii*), positive XP-EHH values indicate longer haplotypes and therefore recent selection in the first population (e.g., BF *gambiae*), and negative XP-EHH values indicate selection in the second population (e.g., BF *coluzzii*).



Supplementary Figure 10. Haplotype structure at metabolic insecticide resistance loci. Plot components are as described for Fig. 5. For both loci, SNPs shown in the lower panel are all either non-synonymous or splice site variants, and are associated with one or more haplotypes under selection. **a**, Haplotype clustering using 1,375 SNPs within the region 3R:28,591,663-28,602,280 spanning 8 genes (*Gste1*-*Gste8*). **b**, Haplotype clustering using 1,844 SNPs within the region 2R:28,491,415-28,502,910 spanning 5 genes (*Cyp6p1*-*Cyp6p5*).

363 References

- 364 1. Noor, A. M. *et al.* The changing risk of Plasmodium falciparum malaria infection in Africa: 2000-
365 10: a spatial and temporal analysis of transmission intensity. *Lancet (London, England)* **383**,
366 1739–47 (2014).
- 367 2. Bhatt, S. *et al.* The effect of malaria control on Plasmodium falciparum in Africa between 2000
368 and 2015. *Nature* **526**, 207–211 (2015).
- 369 3. Hemingway, J. *et al.* Averting a malaria disaster: will insecticide resistance derail malaria control?
370 *Lancet* (2016). doi:10.1016/S0140-6736(15)00417-1
- 371 4. Churcher, T. S. *et al.* The impact of pyrethroid resistance on the efficacy and effectiveness of
372 bednets for malaria control in Africa. *Elife* **5**, 352 (2016).
- 373 5. Gatton, M. L. *et al.* The importance of mosquito behavioural adaptations to malaria control in
374 Africa. *Evolution (N. Y.)*. **67**, (2013).
- 375 6. Raghavendra, K. *et al.* Chlorfenapyr: a new insecticide with novel mode of action can control
376 pyrethroid resistant malaria vectors. *Malar. J.* **10**, 16 (2011).
- 377 7. Oxborough, R. M. *et al.* A new class of insecticide for malaria vector control: evaluation of
378 mosquito nets treated singly with indoxacarb (oxadiazine) or with a pyrethroid mixture against
379 Anopheles gambiae and Culex quinquefasciatus. *Malar. J.* **14**, 353 (2015).
- 380 8. Windbichler, N. *et al.* A synthetic homing endonuclease-based gene drive system in the human
381 malaria mosquito. *Nature* **473**, 212–215 (2011).
- 382 9. Gantz, V. M. *et al.* Highly efficient Cas9-mediated gene drive for population modification of the
383 malaria vector mosquito Anopheles stephensi. *Proc. Natl. Acad. Sci.* 201521077 (2015).

- 384 doi:10.1073/pnas.1521077112
- 385 10. Hammond, A. *et al.* A CRISPR-Cas9 gene drive system targeting female reproduction in the
386 malaria mosquito vector *Anopheles gambiae*. *Nat. Biotechnol.* 1–8 (2015). doi:10.1038/nbt.3439
- 387 11. Tene Fossog, B. *et al.* Habitat segregation and ecological character displacement in cryptic African
388 malaria mosquitoes. *Evol. Appl.* **8**, 326–345 (2015).
- 389 12. Diabate, A. *et al.* Larval development of the molecular forms of *Anopheles gambiae* (Diptera:
390 Culicidae) in different habitats: a transplantation experiment. *J Med Entomol* **42**, 548–553 (2005).
- 391 13. Gimonneau, G. *et al.* A behavioral mechanism underlying ecological divergence in the malaria
392 mosquito *Anopheles gambiae*. *Behav. Ecol.* **21**, 1087–1092 (2010).
- 393 14. Dao, A. *et al.* Signatures of aestivation and migration in Sahelian malaria mosquito populations.
394 *Nature* **516**, 387–90 (2014).
- 395 15. Coetzee, M. *et al.* *Anopheles coluzzii* and *Anopheles amharicus*, new members of the *Anopheles*
396 *gambiae* complex. *Zootaxa* **3619**, (2013).
- 397 16. Torre, A. della *et al.* Molecular evidence of incipient speciation within *Anopheles gambiae* s.s. in
398 West Africa. *Insect Mol. Biol.* **10**, 9–18 (2001).
- 399 17. Lawniczak, M. K. N. *et al.* Widespread divergence between incipient *Anopheles gambiae* species
400 revealed by whole genome sequences. *Science* **330**, 512–4 (2010).
- 401 18. Neafsey, D. E. *et al.* SNP genotyping defines complex gene-flow boundaries among African
402 malaria vector mosquitoes. *Science* **330**, 514–7 (2010).
- 403 19. Aboagye-Antwi, F. *et al.* Experimental Swap of *Anopheles gambiae*'s Assortative Mating
404 Preferences Demonstrates Key Role of X-Chromosome Divergence Island in Incipient Sympatric

- 405 Speciation. *PLoS Genet.* **11**, e1005141 (2015).
- 406 20. Oliveira, E. *et al.* High Levels of Hybridization between Molecular Forms of *Anopheles gambiae*
407 from Guinea Bissau. *J. Med. Entomol.* **45**, 1057–1063 (2008).
- 408 21. Caputo, B. *et al.* The ‘far-west’ of *Anopheles gambiae* molecular forms. *PLoS One* **6**, (2011).
- 409 22. Weetman, D., Wilding, C. S., Steen, K., Pinto, J. & Donnelly, M. J. Gene flow-dependent genomic
410 divergence between *Anopheles gambiae* M and S forms. *Mol. Biol. Evol.* **29**, 279–91 (2012).
- 411 23. Lee, Y. *et al.* Spatiotemporal dynamics of gene flow and hybrid fitness between the M and S
412 forms of the malaria mosquito, *Anopheles gambiae*. *Proc. Natl. Acad. Sci. U. S. A.* **110**, (2013).
- 413 24. Clarkson, C. S. *et al.* Adaptive introgression between *Anopheles* sibling species eliminates a major
414 genomic island but not reproductive isolation. *Nat. Commun.* **5**, 4248 (2014).
- 415 25. Norris, L. C. *et al.* Adaptive introgression in an African malaria mosquito coincident with the
416 increased usage of insecticide-treated bed nets. *Proc. Natl. Acad. Sci.* 201418892 (2015).
417 doi:10.1073/pnas.1418892112
- 418 26. Sharakhova, M. V *et al.* Genome mapping and characterization of the *Anopheles gambiae*
419 heterochromatin. *BMC Genomics* **11**, 459 (2010).
- 420 27. Sharakhova, M. V *et al.* Update of the *Anopheles gambiae* PEST genome assembly. *Genome Biol.*
421 **8**, R5 (2007).
- 422 28. Li, H. & Durbin, R. Fast and accurate short read alignment with Burrows-Wheeler transform.
423 *Bioinformatics* **25**, 1754–60 (2009).
- 424 29. DePristo, M. A. *et al.* A framework for variation discovery and genotyping using next-generation
425 DNA sequencing data. *Nat. Genet.* **43**, 491–8 (2011).

- 426 30. Abecasis, G. R. *et al.* A map of human genome variation from population-scale sequencing.
427 *Nature* **467**, 1061–73 (2010).
- 428 31. The 1000 Genomes Project Consortium. An integrated map of genetic variation from 1,092
429 human genomes. *Nature* **491**, 56–65 (2012).
- 430 32. Delaneau, O., Howie, B., Cox, A. J., Zagury, J.-F. & Marchini, J. Haplotype estimation using
431 sequencing reads. *Am. J. Hum. Genet.* **93**, 687–96 (2013).
- 432 33. Gabriel, S., Ziaugra, L. & Tabbaa, D. SNP genotyping using the Sequenom MassARRAY iPLEX
433 platform. *Curr. Protoc. Hum. Genet.* **Chapter 2**, Unit 2.12 (2009).
- 434 34. Vincenten, N. *et al.* The kinetochore prevents centromere-proximal crossover recombination
435 during meiosis. *Elife* **4**, 923–937 (2015).
- 436 35. Burri, R. *et al.* Linked selection and recombination rate variation drive the evolution of the
437 genomic landscape of differentiation across the speciation continuum of *Ficedula* flycatchers.
438 *Genome Res.* **25**, 1656–65 (2015).
- 439 36. Chan, A. H., Jenkins, P. A. & Song, Y. S. Genome-wide fine-scale recombination rate variation in
440 *Drosophila melanogaster*. *PLoS Genet.* **8**, e1003090 (2012).
- 441 37. Lack, J. B. *et al.* The *Drosophila* Genome Nexus: A Population Genomic Resource of 623
442 *Drosophila melanogaster* Genomes, Including 197 from a Single Ancestral Range Population.
443 *Genetics* genetics.115.174664- (2015). doi:10.1534/genetics.115.174664
- 444 38. Martin, S. H. *et al.* Natural Selection and Genetic Diversity in the Butterfly *Heliconius*
445 *Melpomene*. *Genetics* (2016).
- 446 39. Jinek, M. *et al.* A programmable dual-RNA-guided DNA endonuclease in adaptive bacterial

- 447 immunity. *Science* **337**, 816–21 (2012).
- 448 40. Turner, T. L., Hahn, M. W. & Nuzhdin, S. V. Genomic islands of speciation in *Anopheles gambiae*.
449 *PLoS Biol.* **3**, 1572–1578 (2005).
- 450 41. White, B. J., Cheng, C., Simard, F., Costantini, C. & Besansky, N. J. Genetic association of physically
451 unlinked islands of genomic divergence in incipient species of *Anopheles gambiae*. *Mol. Ecol.* **19**,
452 925–39 (2010).
- 453 42. Fontaine, M. C. *et al.* Extensive introgression in a malaria vector species complex revealed by
454 phylogenomics. *Science* science.1258524- (2014). doi:10.1126/science.1258524
- 455 43. Fanello, C., Santolamazza, F. & Della Torre, A. Simultaneous identification of species and
456 molecular forms of the *Anopheles gambiae* complex by PCR-RFLP. *Med. Vet. Entomol.* **16**, 461–
457 465 (2002).
- 458 44. Coluzzi, M., Sabatini, A., della Torre, A., Di Deco, M. A. & Petrarca, V. A polytene chromosome
459 analysis of the *Anopheles gambiae* species complex. *Science* **298**, 1415–8 (2002).
- 460 45. Stump, A. D. *et al.* Genetic exchange in 2La inversion heterokaryotypes of *Anopheles gambiae*.
461 *Insect Mol. Biol.* **16**, 703–9 (2007).
- 462 46. Davies, T. G. E., Field, L. M., Usherwood, P. N. R. & Williamson, M. S. A comparative study of
463 voltage-gated sodium channels in the Insecta: Implications for pyrethroid resistance in
464 Anopheline and other Neopteran species. *Insect Mol. Biol.* (2007). doi:10.1111/j.1365-
465 2583.2007.00733.x
- 466 47. Alexander, D. H., Novembre, J. & Lange, K. Fast model-based estimation of ancestry in unrelated
467 individuals. *Genome Res.* **19**, 1655–64 (2009).

- 468 48. Lehmann, T. *et al.* The Rift Valley Complex as a Barrier to Gene Flow for *Anopheles gambiae* in
469 Kenya. *J. Hered.* **91**, 165–168 (1999).
- 470 49. Lehmann, T. Population Structure of *Anopheles gambiae* in Africa. *J. Hered.* **94**, 133–147 (2003).
- 471 50. Slotman, M. A. *et al.* Evidence for subdivision within the M molecular form of *Anopheles*
472 *gambiae*. *Mol. Ecol.* **16**, 639–649 (2006).
- 473 51. Pinto, J. *et al.* Geographic population structure of the African malaria vector *Anopheles gambiae*
474 suggests a role for the forest-savannah biome transition as a barrier to gene flow. *Evol. Appl.* **6**,
475 910–24 (2013).
- 476 52. Service, M. W. Mosquito (Diptera: Culicidae) dispersal--the long and short of it. *J Med Entomol*
477 **34**, 579–588 (1997).
- 478 53. Costantini, C. *et al.* Density, survival and dispersal of *Anopheles gambiae* complex mosquitoes in
479 a West African Sudan savanna village. *Med. Vet. Entomol.* **10**, 203–219 (1996).
- 480 54. Marsden, C. D. *et al.* Asymmetric introgression between the M and S forms of the malaria vector,
481 *Anopheles gambiae*, maintains divergence despite extensive hybridization. *Mol. Ecol.* **20**, (2011).
- 482 55. Nwakanma, D. C. *et al.* Breakdown in the process of incipient speciation in *Anopheles gambiae*.
483 *Genetics* **193**, (2013).
- 484 56. Caputo, B. *et al.* The last bastion? X chromosome genotyping of *Anopheles gambiae* species pair
485 males from a hybrid zone reveals complex recombination within the major candidate ‘genomic
486 island of speciation’. *Mol. Ecol.* **25**, 5719–5731 (2016).
- 487 57. Schraiber, J. G. & Akey, J. M. Methods and models for unravelling human evolutionary history.
488 *Nat. Rev. Genet.* **16**, 727–740 (2015).

- 489 58. Liu, X. & Fu, Y.-X. Exploring population size changes using SNP frequency spectra. *Nat. Genet.* **47**,
490 555–559 (2015).
- 491 59. Gutenkunst, R. N., Hernandez, R. D., Williamson, S. H. & Bustamante, C. D. Inferring the joint
492 demographic history of multiple populations from multidimensional SNP frequency data. *PLoS*
493 *Genet.* **5**, e1000695 (2009).
- 494 60. Keightley, P. D., Ness, R. W., Halligan, D. L. & Haddrill, P. R. Estimation of the spontaneous
495 mutation rate per nucleotide site in a *Drosophila melanogaster* full-sib family. *Genetics* **196**, 313–
496 20 (2014).
- 497 61. Schrider, D. R., Houle, D., Lynch, M. & Hahn, M. W. Rates and genomic consequences of
498 spontaneous mutational events in *Drosophila melanogaster*. *Genetics* **194**, 937–54 (2013).
- 499 62. Grollemund, R. *et al.* Bantu expansion shows that habitat alters the route and pace of human
500 dispersals. *Proc. Natl. Acad. Sci. U. S. A.* **112**, 13296–13301 (2015).
- 501 63. Bostoen, K. *et al.* Middle to Late Holocene Paleoclimatic Change and the Early Bantu Expansion in
502 the Rain Forests of Western Central Africa. *Curr. Anthropol.* **56**, 354–384 (2015).
- 503 64. Li, S., Schlebusch, C. & Jakobsson, M. Genetic variation reveals large-scale population expansion
504 and migration during the expansion of Bantu-speaking peoples. *Proc. R. Soc. London B Biol. Sci.*
505 **281**, (2014).
- 506 65. Gignoux, C. R., Henn, B. M. & Mountain, J. L. Rapid, global demographic expansions after the
507 origins of agriculture. *Proc. Natl. Acad. Sci. U. S. A.* **108**, 6044–9 (2011).
- 508 66. Anhof, D. in *Southern Hemisphere Paleo- and Neoclimates* 225–248 (Springer Berlin Heidelberg,
509 2000). doi:10.1007/978-3-642-59694-0_15

- 510 67. Noor, A. M. *et al.* Increasing Coverage and Decreasing Inequity in Insecticide-Treated Bed Net
511 Use among Rural Kenyan Children. *PLoS Med.* **4**, e255 (2007).
- 512 68. McQuillan, R. *et al.* Runs of homozygosity in European populations. *Am. J. Hum. Genet.* **83**, 359–
513 72 (2008).
- 514 69. Purfield, D. C., Berry, D. P., McParland, S. & Bradley, D. G. Runs of homozygosity and population
515 history in cattle. *BMC Genet.* **13**, 70 (2012).
- 516 70. Crawford, J. E. *et al.* Evolution of GOUNDRY, a cryptic subgroup of *Anopheles gambiae* s.l., and its
517 impact on susceptibility to Plasmodium infection. *Mol. Ecol.* (2016). doi:10.1111/mec.13572
- 518 71. O’Loughlin, S. M. *et al.* Genomic signatures of population decline in the malaria mosquito
519 *Anopheles gambiae*. *Malar. J.* **15**, 182 (2016).
- 520 72. Mwangangi, J. M. *et al.* Shifts in malaria vector species composition and transmission dynamics
521 along the Kenyan coast over the past 20 years. *Malar. J.* **12**, 13 (2013).
- 522 73. Mogeni, P. *et al.* Age, Spatial, and Temporal Variations in Hospital Admissions with Malaria in
523 Kilifi County, Kenya: A 25-Year Longitudinal Observational Study. *PLOS Med.* **13**, e1002047
524 (2016).
- 525 74. Garud, N. R., Messer, P. W., Buzbas, E. O. & Petrov, D. A. Recent Selective Sweeps in North
526 American *Drosophila melanogaster* Show Signatures of Soft Sweeps. *PLoS Genet.* **11**, 1–32 (2015).
- 527 75. Sabeti, P. C. *et al.* Genome-wide detection and characterization of positive selection in human
528 populations. *Nature* **449**, 913–8 (2007).
- 529 76. Mitchell, S. N. *et al.* Metabolic and target-site mechanisms combine to confer strong DDT
530 resistance in *Anopheles gambiae*. *PLoS One* **9**, e92662 (2014).

- 531 77. Opondo, K. O. *et al.* Does insecticide resistance contribute to heterogeneities in malaria
532 transmission in The Gambia? *Malar. J.* **15**, 166 (2016).
- 533 78. Müller, P. *et al.* Field-caught permethrin-resistant *Anopheles gambiae* overexpress CYP6P3, a
534 P450 that metabolises pyrethroids. *PLoS Genet.* **4**, e1000286 (2008).
- 535 79. Edi, C. V *et al.* CYP6 P450 enzymes and ACE-1 duplication produce extreme and multiple
536 insecticide resistance in the malaria mosquito *Anopheles gambiae*. *PLoS Genet.* **10**, e1004236
537 (2014).
- 538 80. Pinto, J. *et al.* Multiple Origins of Knockdown Resistance Mutations in the Afrotropical Mosquito
539 Vector *Anopheles gambiae*. *PLoS One* **2**, e1243 (2007).
- 540 81. ETANG, J. *et al.* Polymorphism of intron-1 in the voltage-gated sodium channel gene of
541 *Anopheles gambiae* s.s. populations from Cameroon with emphasis on insecticide knockdown
542 resistance mutations. *Mol. Ecol.* **18**, 3076–3086 (2009).
- 543 82. Lynd, A. *et al.* Field, genetic, and modeling approaches show strong positive selection acting upon
544 an insecticide resistance mutation in *Anopheles gambiae* s.s. *Mol. Biol. Evol.* **27**, 1117–25 (2010).
- 545 83. Mitchell, S. N. *et al.* Metabolic and Target-Site Mechanisms Combine to Confer Strong DDT
546 Resistance in *Anopheles gambiae*. *PLoS One* **9**, e92662 (2014).
- 547 84. Langley, C. H. *et al.* Genomic variation in natural populations of *Drosophila melanogaster*.
548 *Genetics* **192**, 533–98 (2012).
- 549 85. Ross, R. Inaugural Lecture on the Possibility of Extirpating Malaria from Certain Localities by a
550 New Method. *Br. Med. J.* **2**, 1–4 (1899).
- 551 86. de Souza, D. K. *et al.* Filling the Gap 115 Years after Ronald Ross: The Distribution of the

- 552 Anopheles coluzzii and Anopheles gambiae s.s from Freetown and Monrovia, West Africa. *PLoS*
553 *One* **8**, e64939 (2013).
- 554 87. Sayre, R. G. *et al.* A new map of standardized terrestrial ecosystems of Africa. *African Geogr. Rev.*
555 (2013).
- 556